Materials Advances

REVIEW

Check for updates

PEEK implants for cranioplasty: a mapping review of 3D printing, surface functionalisation, and clinical performance gaps

Zoltán Márk Horváth, [ID] [a] Roman Viter, [ID] [b] Oskars Radziņš, [ID] [c] Andreas Thor, [ID] [d] Tetiana Kolisnyk [ID] *[e] and Valentyn Mohylyuk [ID] *[a]

Cranioplasty remains associated with significant intra- and postoperative complications, with infection as the leading cause of implant failure. Autologous bone grafts, in particular, may fail in up to 50% of cases due to bone resorption. These clinical challenges highlight the need for implants that combine mechanical reliability, biocompatibility, and patient-specific precision. Among candidate materials, polyether ether ketone (PEEK) has gained increasing attention, especially when fabricated *via* fused deposition modeling (FDM). The first successful cranioplasty using an FDM 3D-printed PEEK implant was reported in 2022, demonstrating recent clinical translation of this technology. Despite well-documented structural differences between cranial and femoral bones, as well as intra-/interpersonal cranial bone variation, the mechanical properties of 3D-printed PEEK are often benchmarked against femoral bone or averaged values. While the effects of FDM process parameters have been extensively studied, knowledge gaps remain regarding less-explored parameter combinations, printer variability, and their effects on implant performance. Surface functionalisation and drug-loading strategies offer potential to enhance PEEK's bioactivity and antimicrobial properties, yet their mechanical consequences are not fully understood. This mapping review highlights current limitations in the understanding of PEEK cranial implants and emphasises the need for region-specific bone data, systematic evaluation of printing parameters, and integrated functionalisation approaches to optimise implant performance and improve clinical outcomes.

1. Introduction

Modern regenerative medicine has achieved remarkable success in treating a wide spectrum of injuries, from severe traumas caused by residential, industrial, and traffic accidents to military-related wounds, by enabling the restoration of missing bone fragments or components through surgical implants. Patient-specific implants tailored to each patient's unique anatomy dramatically accelerate recovery, reduce complications, and improve quality of life, especially in cases of complex cranial injuries.[1,2]

Cranioplasty, the surgical reconstruction of cranial defects, has evolved from early bone grafts to advanced alloplastic materials. Among current implant options, titanium remains the clinical gold standard due to its strength and biocompatibility, while polymers such as polymethylmethacrylate (PMMA), porous polyethylene, and polyether ether ketone (PEEK) and polyether ketone ketone (PEKK), both from the polyaryletherketone (PAEK) family, are increasingly applied. PEEK, in particular, has gained attention because of its radiolucency, favourable thermal properties, and mechanical compatibility with bone. With the advent of additive manufacturing, three-dimensional (3D) printing, especially FDM†, offers the possibility of fabricating highly customised, patient-specific PEEK cranial implants. Although the mechanical properties of other PAEKs (*i.e.* PEKK) are promising,[3,4] PEEK remains the most widely studied and clinically adopted material for cranial reconstruction owing to its established printability and clinical evidence base.

Despite these advances, cranioplasty still faces significant challenges. Reported complication rates range from 12% to 37%[5–16] with infection as the leading cause[17] and mortality

[a] *Leading Research Group, Faculty of Pharmacy, Rīga Stradiņš University, LV-1007 Riga, Latvia. E-mail: valentyn.mohylyuk@rsu.lv*

[b] *Faculty of Science and Technology, University of Latvia, 19 Raina Blvd, LV 1586 Riga, Latvia*

[c] *Department of Orthodontics, Rīga Stradiņš University, LV-1007 Riga, Latvia*

[d] *Plastic and Oral and Maxillofacial Surgery, Uppsala University, Uppsala, Sweden*

[e] *School of Pharmacy, Queen's University Belfast, Belfast, UK. E-mail: kolisnyktatyana@gmail.com*

† Fused deposition modelling – an additive manufacturing technique where thermoplastic materials are extruded layer by layer to create 3D objects.

rates ranging from 0.5% to 3.2%.[5,12,13] PEEK implants, while clinically established, are limited by their bioinert and hydrophobic nature, which hinders osseointegration and increases infection risk. Strategies such as surface modification and localised drug delivery are being investigated, but their effects on implant performance, particularly in relation to FDM 3D printing, remain insufficiently understood. Moreover, there is no standardised protocol for the design, processing, or clinical implementation of FDM 3D-printed PEEK implants, with current practices relying on local regulations,[18] trial-and-error, and surgeon expertise.

Therefore, the aim of this review is to map the current state of knowledge on FDM 3D-printed PEEK cranial implants, with a focus on: (i) mechanical and physical properties of PEEK compared to cranial bone and titanium; (ii) optimisation of FDM 3D printing parameters; (iii) surface modification techniques for improved bioactivity and osseointegration; (iv) sterilisation methods; and (v) drug-loading approaches for infection control. By mapping and critically summarising the available knowledge on PEEK-based cranial implants, this review aims to contribute to the identification of prospective strategies that may lower mortality and complication rates, enhance mechanical performance, and ultimately improve patients' quality of life.

2. Methodology

A structured mapping review as a literature search strategy was conducted to assess the current state of knowledge regarding FDM 3D-printed PEEK cranial implants. The literature was identified using PubMed, Web of Science/Scopus, and the Google Scholar search engine.

Search terms included combinations of "cranioplasty", "cranial implant", "fused deposition modelling", "fused filament fabrication", "PEEK", "mechanical properties", "physical properties", "titanium", "cranial cortical bone", "surface modification", "osseointegration", and "drug loading", including abbreviations and synonyms. Studies were included if they provided information on FDM 3D-printed PEEK cranial implants or related properties, processing methods, surface modifications, sterilisation, or drug-loading techniques. Studies were excluded if they focused solely on non-cranial applications of PEEK and did not involve FDM or patient-specific implants. Data were synthesised to identify trends in implant performance, 'processing–property' relationships, and surface engineering strategies relevant to clinical outcomes, including infection control and mechanical compatibility.

3. Systematised findings

3.1. Genesis and anatomy of cranial bones

Understanding the developmental origin, structure, and healing patterns of cranial bones is fundamental for designing successful implants. Unlike other skeletal sites, cranial bones possess unique embryological derivation, microarchitecture,
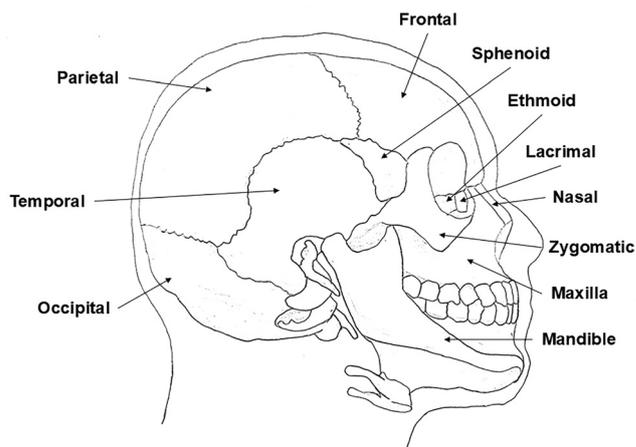

Fig. 1 The anatomy of the human cranial vault (in accordance with ref. 22).

and vascularisation patterns that directly affect their mechanical performance, integration with grafts or synthetic materials, and response to surgical reconstruction. Without accounting for these differences, even advanced biomaterials may fail to replicate the natural biomechanics and regenerative capacity of the cranial vault.

Human cranial bones differ not only by anatomical locations (Fig. 1), but also among individuals due to morphological variations.[19] They also differ significantly from the femoral bone because of their distinct embryological origins, vascularisation, and microstructure.[20,21] These factors lead to variations in their physical and mechanical properties.

Bone formation in humans involves the condensation of mesenchymal cells‡.[22] The mesenchymal cells responsible for the formation of the cranial bones are derived from neural crest cells (i.e. frontal, temporal, sphenoid, ethmoid, lacrimal, nasal, zygomatic, maxilla, and mandible) and the paraxial mesoderm§ (i.e. parietal and occipital) and they undergo intramembranous ossification¶, forming flat membranous bones directly,[22] characterized by a tri-laminar structure with outer and inner cortical layers sandwiching a porous diploë layer.[20,23] In contrast, the mesenchymal cells forming the femoral bone are derived from the lateral plate mesoderm and they undergo chondrification‖ to form a cartilage template**. Endochondral ossification then replaces the cartilage with bone.[24] The intramembranous ossification pathway results in a more diffuse and spatially regulated vascular network, in contrast to the denser, more centralised vascular architecture of endochondral bones such as the femur.[22,24] Recent studies demonstrate that cranial bone

---

‡ A multipotent stromal cell capable of differentiating into bone, cartilage, muscle, and fat tissue.
§ A region of the embryonic mesoderm that gives rise to somites, which develop into skeletal muscle, vertebrae, and dermis.
¶ The direct formation of bone from mesenchymal tissue without a cartilage intermediate.
‖ The process by which mesenchymal cells differentiate into cartilage-forming chondrocytes.
** A temporary cartilaginous structure that guides bone development during endochondral ossification.
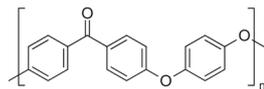
Fig. 2 Molecular structure of PEEK.

vascularisation during healing is temporally uncoupled from osteogenesis: vascular sprouting precedes the migration of bone-forming cells. By contrast, in femoral bone repair, angiogenesis†† and osteogenesis‡‡ are closely synchronised.[25] This highlights region-specific differences in vascular architecture and regenerative strategies, which must inform implant design and evaluation. Experimental data (discussed later) further demonstrate the differences between cranial and femoral bone properties.

3.2. History of cranioplasty: from Xenografts to PEEK and contemporary challenges

The unique embryological origin, morphology, and healing characteristics of cranial bones have always presented challenges for their surgical reconstruction. Unlike long bones, which regenerate more predictably, cranial defects require careful protection of the brain while restoring both mechanical stability and cosmetic appearance. Additionally, the situation is complicated by the fact that cranial bones are relatively thin. These demands explain why cranioplasty, performed to restore the shape and integrity of the cranial bones after various pathologies, injury, previous surgery, or congenital defects, has one of the longest and most diverse histories in surgical practice. This is accompanied by continuous refinement of materials and techniques aimed at reproducing the structural and functional properties of native cranial bone.

The earliest documented description of cranioplasty was given in 1505 by the military surgeon Ibrahim bin Abdullah, describing the repair of a human cranial defect by transplanting bone tissue from non-human species (xenograft).[26] However, the first successful cranioplasty was reported in 1668 by the Dutch surgeon Job Janszoon van Meekeren, who described the case of a nobleman whose cranial defect, inflicted by a sword wound, had been repaired by an unnamed surgeon by xenografting bone tissue from a deceased dog.[27]

The advancement in cranioplasty continued in 1821, when Philipp Franz von Walther reconstructed a part of cranium post-trepanation with bone tissue harvested from the patient's own body (autograft).[28] Since then, autologous bone grafts have been used and harvested from various locations within the body, such as the tibia, ribs, scapula, ilium, and sternum.[29] Cadaveric implantation of allografts was introduced between 1915 and 1919.[29] Xenografts and allografts are no longer preferred in modern cranioplasty due to poor integration, immune reactions, infection risks and inferior outcomes compared to autografts.[30] However, since autograft also presents

challenges, such as a variable resorption rate among patients, the advancement in cranioplasty has shifted towards bone substitutes and synthetic materials.[30–33]

Historically, major advancements in cranioplasty occurred during times of war, as large numbers of traumatic cranial injuries required urgent surgical innovation.[34–36] The increased volume of head trauma cases during World War 1 and 2 catalysed the development and testing of new surgical methods and materials, including the introduction of allografts and metals such as tantalum.[34,37] Wartime exigencies led to rapid experimentation, standardisation, and documentation of surgical approaches to meet the complex needs of traumatic cranial defects caused by blasts and ballistic injuries.[34,35] Subsequently, peacetime adopted and refined these innovations, allowing for more gradual, patient-specific refinements and the integration of newer technologies.[36]

Metallic bone substitutes were used for cranioplasty, including aluminium, gold, stainless steel, platinum, silver, lead, vitallium (Co–Cr–Mo alloy), and tantalum. However due to various disadvantages, technical difficulties, and side effects, most of the metals were unsuccessful.[29,38] While tantalum was most commonly used for cranioplasty during World War II,[37] it fell into disuse due to its high thermal conductivity§§ (57.6 W m^{-1} K^{-1} at 20 °C, linearly increasing with temperature to 61.4 W m^{-1} K^{-1} at 1527 °C[39]). The first metal to show consistently satisfactory results was titanium, which has been in use since 1961.[40] Today, the most commonly used titanium for cranioplasty is grade 5 surgical titanium Ti–6Al–4V alloy[41,42] with a thermal conductivity of 6.8 W m^{-1} K^{-1} at 23 °C (and 7.5 W m^{-1} K^{-1} at 75 °C).[43] Titanium and its alloys remain the clinical gold standard and are currently the only metallic materials in routine use for cranioplasty.[44]

Alongside the development of bone substitutes and synthetic/alloplastic materials, non-metallic options were also explored, such as celluloid in the late 19th century. These were later replaced by acrylics such as polymethylmethacrylate (PMMA)[45] due to their popularisation,[33] which began to substitute tantalum after 1954.[46] In addition to titanium, other materials widely used in current practice include ceramics, such as porous hydroxyapatite (HA)[47] and CaP-formulations with pyrophosphate (monetite-based),[48] and polymers, such as porous polyethylene[49] and polyether ether ketone (PEEK; Fig. 2).[44] The first cranioplasty using the semi-crystalline thermoplastic polymer PEEK was reported in 2007,[50] in which the PEEK cranial implant was prepared *via* binder jetting¶¶. Since then, PEEK has been increasingly applied in clinical practice.[14] In 2022, a successful cranioplasty was reported using a patient-specific PEEK cranial implant fabricated *via* FDM 3D-printing.[51]

---

†† The physiological process through which new blood vessels form from pre-existing vasculature.

‡‡ The formation and development of bone tissue.

§§ Thermal conductivity is a material property that describes how well heat is transferred through a substance. Materials with high thermal conductivity transfer heat quickly and efficiently.

¶¶ Binder jetting is an additive manufacturing technique where an inkjet-style print head selectively deposits a liquid binding agent onto a layer of powder, fusing the particles together to form a three-dimensional object layer by layer.

Recently, alloplastic materials have become the preferred choice for cranioplasty,[52] owing to their superior aesthetic outcomes, particularly in the case of overlying scalp atrophy.[53] Before the use of PEEK, cranioplasty underwent a long developmental pathway involving technologies and materials (Fig. 3).

Consequently, modern implant selection is guided by a set of critical properties that dictate clinical outcomes (Table 1).
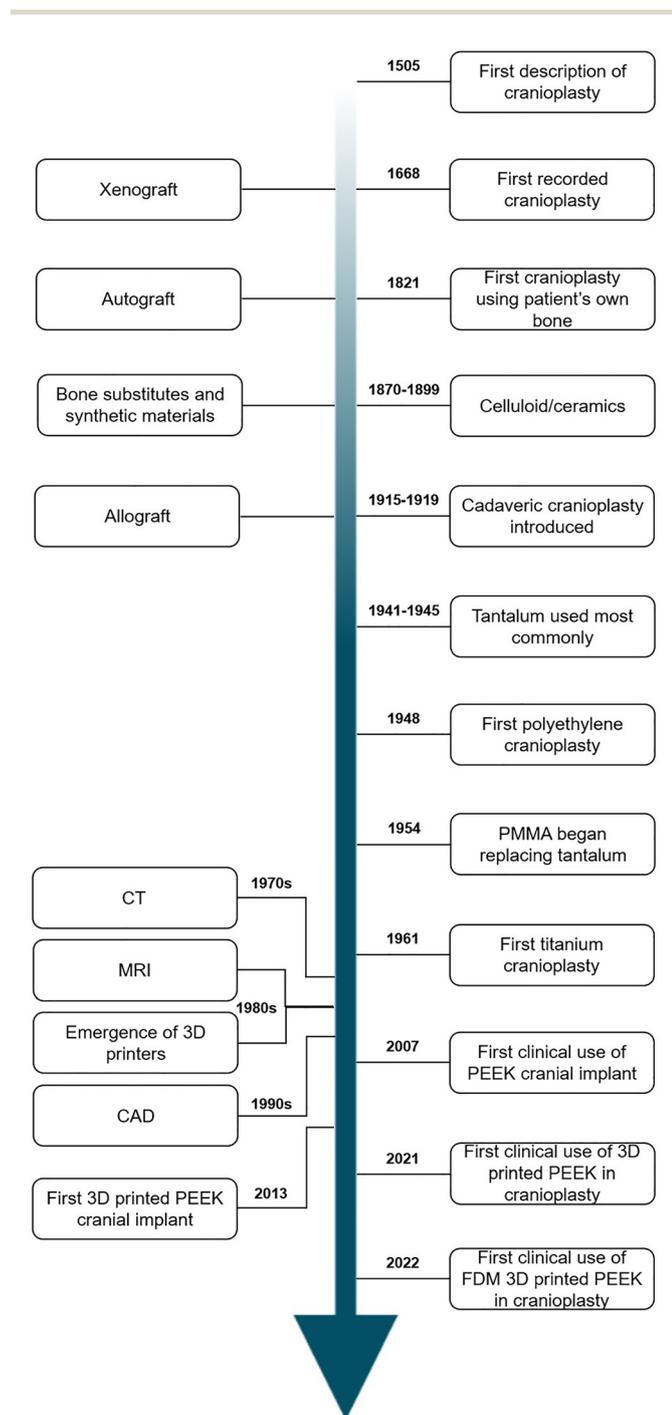

Fig. 3 Cranioplasty timeline.

3.3. PEEK as a cranial implant material and physical properties of PEEK

PEEK is widely regarded as a particularly promising material for patient-specific cranial implants, owing to its distinctive combination of physical and mechanical properties. These properties confer an advantageous balance of strength, low density, and biomechanical compatibility with native cranial bone. The ensuing sections will provide a detailed examination of these characteristics.

The density of conventionally manufactured PEEK is typically around 1.3 g cm^{-3}.[60,69–73] Since density contributes to material stiffness, achieving biomechanical compatibility requires the implant's density to closely match that of the patient's native cranial cortical bone,[59] which ranges from approximately 1.468 to 1.922 g cm^{-3}.[20,74,75] This range varies depending on individual factors such as age, sex, and the anatomical location within the cranial vault.[20,74,76]

The density of PEEK changes with varying 3DP processing parameters.[77] Cranial implants that have higher stiffness‖‖ than the surrounding bone tissues absorb more stress, resulting in osteopenia*** of the surrounding bone tissues (stress shielding).[78,79] PEEK with a density value closer to the range of cranial cortical bone shows better biomechanical compatibility††† than Ti–6Al–4V with a density of 4.43 g cm^{-3}.[43]

The thermal properties of PEEK have been widely studied, with glass transition temperature (T_g) in the range of 143–151 °C,[73,80–82] melt temperature (T_m) between 335 and 343 °C,[60,80–83] and a theoretically calculated melting enthalpy of 100% crystalline PEEK of 130 J g^{-1}.[81] The onset degradation temperature (T_d) has been reported to be in the range of 564–580 °C.[60,84] Variations in these values can be attributed to variations in differential scanning calorimetry (DSC) as well as weight, degree of crystallinity‡‡‡ (DOC), and processing history. The DOC is commonly calculated using DSC as the ratio of the sample's measured melting enthalpy to the theoretically calculated melting enthalpy of 100% crystalline PEEK§§§.[81,85,86]

It is important to ensure that the cranial implant has a relatively low thermal expansion,[60] ideally similar to that of the human cranial cortical bone to avoid disproportional changes in thickness between the cranial implant and the surrounding bone tissues during temperature fluctuations, thereby reducing implant failure risks, such as loosening of the implant or pain. The coefficient of linear thermal expansion (CLTE) of PEEK between room temperature (RT) and its T_g has been reported to

---

‖‖ Stiffness refers to a material's resistance to deformation under an applied load. It is commonly represented by Young's modulus.

*** A condition characterised by lower-than-normal bone mineral density, often a precursor to osteoporosis.

††† Biomechanical compatibility describes how closely the mechanical properties of an implant material match those of the host biological tissue.

‡‡‡ The DOC in a polymer like PEEK refers to the proportion of its molecular chains that are arranged in a highly ordered, crystalline structure, as opposed to an amorphous (disordered) phase.

§§§ 100% fully crystalline PEEK refers to the theoretical state in which all polymer chains are perfectly ordered in a crystalline structure.

Table 1 Key properties of cranioplasty implants and their clinical relevance

Category	Implant property	Clinical relevance	Target/benchmark	Ref.
Geometrical	Implant curvature and contour	Ensures anatomical fit and aesthetic outcome	Patient-specific CAD design based on 3D CT	42
	Thickness	Provides mechanical protection and mimics native skull anatomy	Match native skull thickness (site dependent)	54
	Defect topology replicability	Enables precise fit for complex defects	High-resolution CT imaging	55
Mechanical	Mechanical strength	Prevents fracture under impact or physiological loading	Similar to cranial bone (site/patient dependent)	56
	Young's modulus	Minimises stress shielding, optimises load transfer		57
	Poisson's ratio	Influences deformation under load		58
	Yield stress	Determines the limit before permanent deformation		54
Physical and thermal	Density	Affects implant weight and mechanical compatibility	Similar to cranial bone (site/patient dependent)	59
	Coefficient of thermal expansion	Minimises mismatch with bone to prevent interface stress	Similar to cranial bone	60
	Specific heat capacity	Maintains thermal equilibrium with surrounding tissues		61
	Thermal conductivity	Ensures matching heat transfer with bone to avoid local hot/cold spots	Similar to cranial bone or lower	37
	Thermal stability	Maintains structural integrity during sterilisation and surgical handling	T_g > sterilisation and handling temperature	62
Biological	Biocompatibility	Prevents adverse immune or inflammatory reactions	ISO 10993 compliant[a]	63
	Osseointegration	Promotes long-term stability through bone ingrowth	Porous surface and bioactive coating	64
	Antimicrobial options	Reduces risk of implant associated infection	Antimicrobial coatings	65
Imaging-related	Radiolucency	Facilitates clear post-operative imaging (CT/MRI)	Non-metallic materials preferred	66
	Electrical resistivity	Ensures MRI safety and prevents artefacts	High resistivity	67
Sterilisation	Sterilisability	Required for surgical applications	Compatible with accepted sterilisation methods	68

[a] The ISO 10993 set entails a series of standards for evaluating the biocompatibility of medical devices to manage biological risk.

be in the range of 40–60 × 10^{-6} K^{-1}.[87,88] Although data on the thermal properties of human cranial cortical bone are limited, comparisons are often drawn to femoral cortical bone, which shows a CLTE of 27.5 × 10^{-6} K^{-1} between RT and 65 °C.[89] Notably, the DOC significantly affects the CLTE of PEEK above its T_g but has a minimal influence below it.[90] As a reference, Ti–6Al–4V exhibits a CLTE of 8.6 × 10^{-6} K^{-1} between 20 °C and 100 °C.[43]

The specific heat capacity¶¶¶ of cranial implant materials plays a critical role in maintaining thermal equilibrium with the surrounding bone tissues by minimising temperature fluctuations.[61] The specific heat capacity of PEEK increases from 1.05 to 1.125 J g^{-1} K^{-1} as the temperature rises from 19 °C to 48 °C.[91] In comparison, human femoral cortical bone shows a specific heat capacity of 1.14 to 1.64 J g^{-1} K^{-1}, as determined using hot water calorimetry‖‖‖.[92] This measurement reflects the heat exchange between bone samples initially at approximately 20 °C and water initially near 70 °C, with specific heat calculated based on the resulting equilibrium temperature (typically between 30 °C and 50 °C). The specific heat capacity of Ti–6Al–4V increases from 0.544 to 0.569 J g^{-1} K^{-1} between 20 °C and 95 °C.[43,93] It should be noted that these measurements were performed over different temperature ranges; therefore, direct comparison between PEEK, human femoral cortical bone, and Ti–6Al–4V values may not fully reflect their relative thermal behaviour under identical physiological

conditions. Nonetheless, the specific heat values of PEEK are generally closer to those of bone, suggesting that it may help maintain thermal equilibrium with the surrounding bone tissues more effectively.

The importance of thermal conductivity was highlighted *via* a clinical outcome and complication study on the use of tantalum in cranioplasty.[37] It was found that the high thermal conductivity of tantalum (57.6 W m^{-1} K^{-1} at 20 °C, linearly increasing with temperature to 61.4 W m^{-1} K^{-1} at 1527 °C[39]) led to patient discomfort due to heat or cold sensitivity at the implant site.[37] In contrast, PEEK shows lower thermal conductivity, increasing from 0.244 to 0.277 W m^{-1} K^{-1} between 28 °C and 250 °C.[91] Femoral cortical bone, by comparison, exhibits a thermal conductivity of 0.16 to 0.24 W m^{-1} K^{-1} between 30 °C and 55 °C,[92] placing PEEK within a similar range. Meanwhile, Ti–6Al–4V exhibits a significantly higher thermal conductivity of 6.8 W m^{-1} K^{-1} at 23 °C and 7.5 W m^{-1} K^{-1} at 75 °C,[43] which may contribute to greater thermal sensitivity when used in cranial applications.[94]

The electrical resistivity**** of an implant material should be considered regarding imaging compatibility.[67] Magnetic resonance imaging†††† (MRI) scans can induce eddy currents‡‡‡‡ in metallic implants due to the low electrical resistance of metals, causing localised hotspots from where the heat may

---

¶¶¶ Specific heat capacity is the amount of heat energy required to raise the temperature of one gram of a material by one degree Celsius.

‖‖‖ A thermal analysis method that measures the heat of a reaction or material by observing temperature changes in water.

**** Electrical resistivity is a measure of a material's resistance to the flow of electric current.

†††† A non-invasive imaging method that uses strong magnetic fields and radio waves to produce detailed images of soft tissues.

‡‡‡‡ Eddy currents are circulating electrical currents induced in conductive materials when exposed to changing magnetic fields, such as during MRI scanning.

transfer to the surrounding tissues, potentially causing burns.[67] Compared to Ti–6Al–4V, which has a reported electrical resistivity of 1.469×10^{-8} Ω cm at 19.65 °C increasing to 1.501×10^{-8} Ω cm at 75.75 °C,[43] PEEK offers greater imaging compatibility due to its excellent insulating properties, demonstrated by its electrical resistivity of 10^{16} Ω cm.[73]

3.4. Mechanical properties of PEEK

Injection moulded pure PEEK has reported Young's modulus§§§§ values in the range of 3.7–4.15 GPa[73,95–99]; however, this range widens with the lower range reaching 2.415 GPa upon FDM-3DP of PEEK with various factors, such as the nozzle temperature, printing speed, bedplate¶¶¶¶ and chamber‖‖‖‖ temperature, and layer height*****.[100] Furthermore, even broader ranges were obtained by varying the infill angle†††† (2.53–4.27 GPa), applying additional heat treatment (2.53–4.74 GPa), and reducing the nozzle diameter (*i.e.*, from 0.6 mm to 0.4 mm increased Young's modulus from 4.74 to 8.06) for heat-treated samples that were FDM 3D-printed with an infill angle of 180°.[98]

The Young's modulus of PEEK is comparable to that of human cranial cortical bone, which ranges from 2.032 to 21 GPa,[19,74,75,101,102] depending on age, sex, and anatomical location. Biomechanical compatibility – the extent to which an implant mimics the mechanical properties of the surrounding bone tissues – is a critical requirement in cranioplasty. A mismatch in stiffness can lead to stress shielding, potentially resulting in bone resorption, implant loosening, or long-term failure. Compared to conventional Ti–6Al–4V, which has a much higher Young's modulus (110–114 GPa),[43,103,104] PEEK offers superior biomechanical compatibility, promoting more natural load distribution and improved long-term integration.

It is important to characterise the deformation properties of cranial implants, such as Poisson's ratio‡‡‡‡‡ and yield stress§§§§§, because these properties determine how the material responds under physiological loads and deforms in relation to the surrounding bone tissue. Prior to the fabrication of cranial implants *via* FDM 3D printing with the precise shape of the cranial defect, a low yield stress was advantageous for effective shaping of the cranial implant during surgery.[57]

---

§§§§ Young's modulus (also known as elastic modulus) is a measure of a material's stiffness – how much it resists deformation under tensile or compressive stress.

¶¶¶¶ The bedplate, or build plate, in FDM 3DP is the surface on which the printed object is constructed.

‖‖‖‖ An enclosed environment surrounding the build area of a FDM printer, designed to maintain controlled temperature and airflow for optimal print quality and material performance.

***** Layer height in FDM 3DP refers to the vertical thickness of each deposited layer of the material.

†††† The infill angle in FDM 3DP refers to the orientation of the internal fill pattern relative to the print direction.

‡‡‡‡‡ Poisson's ratio is a material property that describes how much a material deforms in directions perpendicular to the applied force, relative to the deformation in the direction of the force.

§§§§§ Stress (pressure) at which the material begins to deform plastically, usually related to the maximum allowable load.

However, these deformation properties of the 3D-printed cranial implants have been neglected, justified by the assumption of low physiological loads on the cranial bone in everyday life. Regardless, the cranial bone may be subjected to physiological load either accidentally or through numerous recreational activities, which highlights the importance of such properties. Ideally the implant should have a Poisson's ratio close to that of the surrounding bone tissue to improve biomechanical compatibility by minimising interfacial stress concentrations.[58] PEEK's Poisson's ratio has been reported to be in the range of 0.380–0.388 for filaments,[97,105] 0.385 for injection moulded forms,[106] and 0.375 to 0.38 for extruded samples.[107,108] In comparison, Ti–6Al–4V shows a range of 0.26–0.36.[43] While the human cranial bone has a mean Poisson's ratio of 0.19,[109] studies have reported a statistically significant variation in the Poisson's ratio of the human cranial cortical bone depending on the anatomical location in the cranial vault (*e.g.* parietal, frontal, occipital, temporal, and zygoma; Fig. 1).[20,110] The yield stress is usually measured under tension for metals and polymers (uniform materials), whereas under shear for bones and composites. The tensile yield stress¶¶¶¶¶ of PEEK ranges from 100 to 110 MPa,[97,99,106] though it can fall below 100 MPa after FDM 3D printing.[111] For Ti–6Al–4V, the tensile yield stress was reported to be in the range of 724–938 MPa.[43] In contrast, the shear yield stress‖‖‖‖‖ of human cranial cortical bone is much lower, reported to be in the range of 51.3–65.3 MPa.[112] In order to evaluate the structural performance of cranial implants, finite element analysis****** (FEA) is commonly used[99,113–115] for the simulation of various physiological loads and the calculation of a theoretical value known as the von Mises stress. The properties of the implant material, its dimensional parameters, the anatomical characteristics of the human skull, and the applied loading conditions are input into the FEA model to perform this analysis. The resulting von Mises stress is then compared to the yield stress obtained from mechanical testing to assess the risk of permanent deformation. If the von Mises stress exceeds the material's yield stress, it indicates likely permanent deformation. In cranioplasty, it is essential to ensure that von Mises stresses in both the implant and the surrounding bone remain below their respective yield stress to avoid complications such as structural failure, implant loosening, or bone resorption. However, stress-based criteria alone may not fully describe failure risk in complex biological structures such as the skull. Cortical bone is an anisotropic composite material, and failure often occurs through crack initiation and propagation rather than uniform yielding, as demonstrated in fracture resistance studies of human cortical bone.[116,117] Therefore, advanced FEA approaches that incorporate fracture mechanics principles such as extended finite element methods for crack growth simulation[118] may provide

---

¶¶¶¶¶ Tensile yield stress is the amount of uniaxial tensile stress required to cause a material to begin permanent (plastic) deformation.

‖‖‖‖‖ Shear yield stress is the stress level at which a material begins to plastically deform under shear loading.

****** A computational technique used to simulate how structures respond to external forces, heat, and other physical effects.

Table 2 Summary of physical and mechanical properties

Property	PEEK	Human cranial cortical bone	Human femoral cortical bone	Ti–6Al–4V
Density, g cm^{-3}	1.3	1.468–1.922	1.834–2.027[121]	4.43
T_g, °C	143–151	N/R	N/R	N/A
T_m, °C	335–343	N/A	N/A	1605–1635[43]
T_d, °C	564–580	220[122]	N/R	N/R
CLTE, 10^{-6} K^{-1}	40–60 (RT – T_g)	N/A	≈27.5 (RT – 65 °C)	8.6 (20 °C–100 °C)
Specific heat capacity, J g^{-1} K^{-1}	1.05–1.125 (19–48 °C)	N/A	1.14–1.64 (30–50 °C)	0.544–0.569 (20–95 °C)
Thermal conductivity, W m^{-1} K^{-1}	0.244–0.277 (28–250 °C)	N/A	0.16–0.24 (30–55 °C)	6.8–7.5 (23–75 °C)
Electrical resistivity, Ω cm	10^{16}	N/A	10^8 (ref. 123 and 124)	1.469 × 10^{-8}–1.501 × 10^{-8} (19.65–75.75 °C)
Young's modulus, GPa	2.415–8.06	2.032–21	9.55–19.9[125–127]	110–114
Poisson's ratio	0.375–0.388	0.19	0.37[125]	0.26–0.36
Tensile yield stress, MPa	100–110	N/A	50–107.9[126,127]	724–938
Shear yield stress, MPa	N/A	51.3–65.3	N/A	N/A

N/A: not available; N/R: not relevant.

deeper insight into crack formation. A critical observation has been made regarding the material properties used in FEA studies. As highlighted previously, PEEK properties change upon 3D printing; however, properties of untreated PEEK and/or values from previous research are often applied in FEA studies.[114,115,119] Likewise, although differences have been documented in cortical bone properties across various anatomical locations of the cranial vault, between individuals, and between cranial and femoral bone, many studies still use either average skull property values, femoral proxy values, or values of unspecified origin.[114,115,119,120] To achieve reliable simulation outcomes, the input material properties must accurately represent the actual, site-specific, and processing-dependent characteristics of both the implant and the surrounding bone (Table 2).

3.5. FDM 3D printing of patient-specific cranial PEEK implants

Three-dimensional (3D) printing, a form of additive manufacturing, has revolutionised the creation of patient-specific implants.[2,41] While 3D bioprinting has been predominantly applied to the fabrication of soft tissue constructs,[128] FDM – also known as fused filament fabrication (FFF) and originally developed by Scott Crump in 1988[129] – has primarily been employed for the additive manufacturing of hard tissue implants. FDM enables the layer-wise extrusion of thermoplastics directly from computer-aided design††††† (CAD) models, based on data obtained from the computed tomography‡‡‡‡‡‡ (CT)/MRI scans.[130]

Although PEEK has been used clinically in cranioplasty since 2007, the recent shift toward additive manufacturing (3D printing) has renewed interest in PEEK, owing to its exceptional thermal, physical, and mechanical properties. The preparation of PEEK cranial implants typically begins with patient-specific imaging, such as CT scan, followed by the generation of a 3D digital model of the defect and surrounding skull anatomy. The work up and design are discussed in collaboration between the treating surgeon and medical engineers/designers, with all clinical contributing data at hand. Based on this model, the cranial implant is then fabricated using various methods. Traditionally, subtractive manufacturing has been predominantly used to produce PEEK cranial implants, such as computer numerical control§§§§§§ (CNC) machining where a solid block of PEEK is milled (i.e., the material is gradually removed by a rotating cutting tool) to match the required geometry.[1,50,131] Although injection moulding – where the molten material is injected into a mould under high pressure – has been employed to produce cranial implants,[132,133] to the best of our knowledge, it has not been reported specifically for PEEK cranial implants, likely due to the material's high processing temperature, extended cycle times, and associated costs regarding PSI. Since 2012, additive manufacturing techniques such as 3D printing have gained increasing attention for the development of medical implants,[134] including the fabrication of cranial implants using PEEK via FDM-based 3D printers,[51,135,136] along with their clinical applications.[51] FDM-based 3D printing requires the material feedstock to be in filament form, which for PEEK is commonly produced through extrusion¶¶¶¶¶¶.[137,138] This technique is particularly advantageous in cranioplasty, since each implant must conform precisely to patient anatomy in terms of curvature, thickness, and defect topology among other properties (Table 1).

The first successful cranioplasty carried out using FDM 3D-printed PEEK was reported in 2022.[51] Prior to the clinical application of the FDM 3D-printed PEEK, it was tested for Young's modulus (3.45 GPa), tensile strength (96 MPa), flexural

---

††††† The use of computer software to create, modify, and optimise detailed design models of objects or structures.

‡‡‡‡‡‡ An imaging technique that uses X-rays and computer processing to generate cross-sectional views of the body.

§§§§§§ A subtractive manufacturing process where computer-guided tools shape materials into precise forms.

¶¶¶¶¶¶ A process where heated thermoplastic is forced through a die to form continuous filaments used in 3D printing.

strength‖‖‖‖‖‖ (154 MPa), and impact toughness******* (80 kJ m^{-2}), which were compared to the average values of a skull from previous studies, without distinguishing between different regions of the cranial vault. Although the authors paid great attention to the thickness of the cranial implant, in order to achieve optimal biomechanical compatibility with the surrounding bone tissues, one must consider the differences in the physical and mechanical properties of the human cranial cortical bone at different regions of the cranial vault.[20]

In addition to literature analysis, process parameters were documented from a representative case example. In this workflow, a 3D model of the cranial defect is designed from patient CT data, with edge thickness measured at approximately 1 mm intervals to replicate the cortical–diploë–cortical structure, and the implant's central thickness matched to the contralateral skull. Fixation holes are integrated for intraoperative convenience under corresponding surgeon guidance. Printing employs a dried PEEK filament (4 hours at 120 °C followed by a retained temperature of 60 °C until printing), fed through a heated oven to an FFF printer with a calibrated perforated bedplate (170 °C for the first layer and 180 °C for the subsequent layers), controlled chamber temperature (90–150 °C), nozzle at 485 °C (0.4 mm diameter), 2000 mm min^{-1} print speed, 45° printing angle, and 100% infill (0°/90°). Given the two approaches of surgical fixation of cranial implants, integrated and non-integrated, with potential benefits of each approach,[139] surgical fixation employs non-integrated titanium plates (<0.5 mm) and screws, with approximately one cranioplasty procedure conducted in Latvia every 3 to 4 months.

It has been demonstrated that FDM printing parameters influence the properties of 3D-printed PEEK. For instance, the tensile strength and density of PEEK were shown to increase rapidly as the nozzle temperature rose from 380 °C to 420 °C, with a slower increase until 440 °C.[140] At lower temperatures such as 380 °C, incomplete melting and limited molecular diffusion led to the formation of voids and visible filament outlines (higher surface roughness) in scanning electron microscopy images. In contrast, printing at 440 °C resulted in improved fluidity, better interlayer bonding, and fewer voids, contributing to increased apparent density and mechanical performance. Increasing the crystallinity increased the Young's modulus and the yield strength of PEEK.[140,141] Furthermore, increased chamber temperature (from 25 °C to 200 °C) was shown to raise the DOC of PEEK from 17% to 31%, thereby improving mechanical properties such as peak force††††††, Young's modulus, and tensile strength.[86] In contrast, increased bedplate temperature (from 100 °C to 130 °C) has enhanced the interlayer adherence which in turn has led to a greater

crystallisation rate, also contributing to improved mechanical performance.[142] Additionally, the large size of cranial implants requires additional focus on homogenous heat distribution to achieve isothermal crystallisation of PEEK.[142] These studies show clear effects of thermal control during and after printing, allowing the tailoring of PEEK crystallinity and thus the mechanical properties of PEEK cranial implants.

The most common nozzle diameter used in FDM 3D printing is 0.4 mm.[77] While the nozzle diameter does not affect the temperature distribution of the printing head (measured at 380 °C), it can influence how the printing speed affects the quality of printed PEEK.[140] A layer thickness of 0.15 mm is recommended for good surface quality,[143] that is, to minimise surface roughness, characteristic lines created by each filament path, gaps, overlaps, and inconsistencies in the deposited material pattern. Furthermore, the printing orientation was demonstrated to affect the mechanical properties of the 3D-printed PEEK due to different degrees of interfacial adhesion.[144–146] Additionally, the importance of printing speed and filling direction was highlighted through the comparison of two studies,[77] showing that 3D-printed PEEK had a higher apparent density and tensile strength with a lower printing speed (1200 mm min^{-1} as compared to 2400 mm min^{-1}), likely due to the additional time each deposited layer had to bond and crystallise.

The annealing temperature during processing and time influence the crystallinity content of PEEK and therefore its thermomechanical properties.[90,147] 3D printing process parameters, such as printing temperature, speed, and nozzle diameter, impact PEEK phase composition (amorphous-to-crystalline state ratio) and thus the physical properties, such as density and surface roughness, and mechanical properties, such as elasticity, plasticity, and tensile strength.[140,142]

3.6. Post-processing – surface modification

The surface modification of PEEK is an important process for the proper integration of PEEK implants with the surrounding tissues.[148] Surface-modifying processes, such as polishing/abrasion and plasma treatment, enable them to properly interact with body tissues and have the potential to alter the qualities of the final medical device. Since the cranial bone is very thin, with thickness in the range of 4.43–8.61 mm,[19,149] positioned directly over the delicate brain tissue, designing the cranial implants with mechanical compatibility is crucial. Due to this intimate proximity and limited thickness, even minor deformations or mechanical failures in the implant or reconstructed bone can transmit stress to neural structures, posing a risk of causing injury or impaired neural function. Additionally, given the mechanical properties of cranial implants at such small thicknesses, it is especially important to closely mimic the cranial bone's mechanical properties to prevent stress shielding or damage. If the implant is too stiff, it can cause stress concentrations leading to bone resorption or implant loosening,[150] whereas overly flexible implants may not offer sufficient protection against impact. Furthermore, the thickness of the cranial bone changes due to aging;[151]

‖‖‖‖‖‖ Flexural strength is the material's ability to resist deformation or fracture when subjected to bending forces.

******* Impact toughness is the material's ability to absorb energy and resist fracture when subjected to sudden or dynamic forces, such as accidental head trauma or impact injuries.

†††††† Peak force is the maximum load or force the implant can withstand before failure or fracture occurs during mechanical tests, such as compression or impact tests.

therefore, it may be important to consider the changing nature of the skull.

Various surface modifications of PEEK have been investigated to enhance its bioactivity for improved osseointegration, as well as to introduce antimicrobial functionality for cranial implants. Highly roughened surfaces – most likely due to the increased surface area – support the metabolic activity and proliferation of osteoblasts‡‡‡‡‡‡‡,[152] which accelerates bone ingrowth and osseointegration.[153] Due to osseointegration resulting from the mechanical interlocking between the implant and the surrounding bone tissues, the implant is often beneficially designed to be porous, either porous-coated or fully porous for cranial implants.[64]

Two significant drawbacks of PEEK as a cranial implant material are its lack of intrinsic antibacterial properties[14,154] and its bioinert and hydrophobic nature, leading to poor osseointegration.[155] Therefore, it is essential to develop bioactive PEEK implants that enhance integration with both soft and bone tissues, promote vascularisation, reduce the risk of microbial contamination, and ultimately improve clinical success rates. A wide range of surface modification techniques have been developed. Common techniques include sandblasting, which creates an irregular surface[156] and increases the surface roughness to enhance physical bonding strength[157] and shear bond strength.[156,158] Plasma treatment grafts atoms or ions – based on the gases used – onto the substrate (PEEK) to increase hydrophilicity and physical bonding strength.[159–161]

Most surface modification of PEEK is based on the cleavage of the C=O bond in the polymer backbone, followed by the formation of new functional groups, such as –OH, COO⁻, and –COOH.[148,162] This process requires significant energy; therefore, conventional ultraviolet (UV) treatment using a mercury lamp is insufficient to achieve effective modification.[162] Variations in the atmosphere, UV light intensity, photon energy and gas partial pressure are key parameters for effective surface modification. The PEEK surface can be effectively oxidised by using a combination of vacuum ultraviolet radiation and an oxidising gas.[163] Although UV irradiation has been applied to increase adhesive bond strength,[164,165] UV-based methods require specific equipment and have limitations regarding the oxidation of large PEEK surfaces.

Accelerated neutral atom beam (ANAB) technology has been employed to enhance the bioactivity of PEEK by creating nano-textured surfaces that improved its hydrophilicity, osteoblast adhesion, proliferation, and differentiation§§§§§§§ without altering the chemical composition of the surface and the mechanical properties of PEEK.[166,167] These findings suggest that ANAB-modified PEEK surfaces can promote better integration with bone tissue, potentially improving the performance of PEEK-based cranial implants.

Sodium hydroxide etching introduces hydroxyl anions to enhance the hydrophilicity and provide nucleation and coating development sites.[168,169] Acid etching can introduce various functional groups depending on the acid used, such as fluorination with hydrofluoric acid[170] or sulphonation with sulphuric acid.[171] Sulphonation not only corrodes the surface of PEEK but also increases surface roughness and generates interconnected nanoporous networks, thereby enhancing shear bond strength.[156,172] Sulphonation is typically performed by brief exposure of PEEK to concentrated sulphuric acid. X-ray diffraction analysis showed no changes in the crystalline structure of FDM 3D-printed PEEK after sulphonation.[172] The contact angle¶¶¶¶¶¶¶ of sulphonated PEEK increased slightly from 65° to 74°, while the mechanical properties remained unaffected. The high porosity of sulphonated PEEK improved biocompatibility despite the higher contact angle. X-ray photoelectron spectroscopy∥∥∥∥∥∥∥ (XPS) and Fourier transform infrared (FTIR) spectroscopy******** confirmed the incorporation of –HSO₃ groups into the PEEK structure.[173] However, the anticipated improvement in wettability was not achieved, indicating that sulphonation should be combined with other oxidation methods.

Laser-based methods are effective for modifying the morphology of PEEK surfaces.[174,175] Interaction with the laser beam induces surface etching and ablation, resulting in highly roughened morphologies.[174,175] CO₂ laser machining has been reported to engrave surface lines to improve cell adhesion and proliferation,[171] while Nd:YVO₄ laser groove treatment enhances shear bond strength.[176] Laser parameters, particularly pulse duration and energy, play critical roles in determining surface properties.[177] For example, ultrashort femtosecond laser treatment enabled the formation of micropatterns on PEEK surfaces, although without substantial improvement in wettability.[178,179]

PEEK treated with a nanosecond laser (1065 nm, 10 W, 4 ns pulse duration) exhibited an enhanced surface roughness (from 0.63 μm to 19.08 μm),[180] without detectable changes in chemical composition. Subsequent integration of HA with a particle size of ≈30 nm into the laser-treated PEEK surface resulted in a contact angle of about 1.3°, and the resulting HA-PEEK demonstrated significantly improved properties for cell growth and bone regeneration.[180]

The effect of laser wavelength on the properties of PEEK has been investigated using pulsed nanosecond lasers at 355, 532, and 1064 nm.[181,182] Due to differences in the absorption coefficient of PEEK, laser ablation††††††† was observed at 532 nm. Treatment at 1064 nm produced a porous surface

---

‡‡‡‡‡‡‡ The cells that form new bones and grow and heal existing bones.
§§§§§§§ The process by which osteoblast precursor cells develop into mature bone-forming cells with specialised functions, such as producing the bone matrix and mineralising.

¶¶¶¶¶¶¶ The angle formed at the interface where a liquid droplet meets a solid surface.
∥∥∥∥∥∥∥ A surface sensitive technique that measures the elemental composition and chemical states of atoms by detecting electrons emitted after X-ray irradiation.
******** A technique that identifies chemical bonds and functional groups by measuring absorption of infrared light at characteristic wavelengths.
††††††† A process in which high-intensity laser irradiation removes material from a solid surface through melting, evaporation, or sublimation.

morphology, while 355 nm irradiation did not markedly alter the surface structure of PEEK. However, improved wettability was achieved with both 1064 nm (through morphological changes) and 355 nm (likely through the formation of polar groups).[181,182]

The effects of laser power on the properties of PEEK have also been investigated.[183,184] PEEK treated with a nanosecond laser (355 nm, 0–5 W, 10 ns pulse duration) showed that increasing power (in the range of 0–5 W) significantly influenced surface roughness and wettability. Indeed, higher laser power resulted in the formation of smaller surface features, enhanced roughness, and reduced contact angle. X-ray diffraction analysis revealed the formation of an amorphous phase, while XPS indicated a crystalline-to-amorphous transition accompanied by the generation of surface –OH groups. FTIR spectra displayed peaks at 1183, 1216, and 1650 cm^{-1}, corresponding to –O–, C–O and C=O functional groups, respectively. Both structural and chemical modifications account for the reduced contact angle. The key factor for improved wettability is the inner hydrophilic surface.

HA has been successfully hydrothermally grown on laser-treated PEEK. It was observed that laser treatment improved the growth of HA during hydrothermal synthesis and its active surface area.[183]

Therefore, laser treatment of the PEEK surface can effectively alter its morphology and wettability. Laser treatment may serve as an alternative to sulphonation; however, to increase the surface concentration of the oxygen species, it is recommended to combine laser treatment with plasma treatment.

Plasma treatment is a well-established method for modifying PEEK surfaces.[185] This modification method mainly involves thermal effects, the substitution of the polymer atoms by atoms from the plasma, the alteration of polymer chains, polymer etching and cross-linking. These processes result in changes to the surface morphology, variations in mechanical properties such as elasticity, and a reduced water contact angle, thereby increasing surface hydrophilicity.[185]

The effects of temperature on PEEK stability during plasma treatment have been investigated.[186] When PEEK is treated with high-power plasma at temperatures exceeding 151 °C a reduction in crystallinity can occur from the surface to the core (up to 300 μm). Such changes may pose a risk of significant mechanical weakening of the PEEK material.

The effects of plasma treatment under different oxidising atmospheres were investigated, where PEEK was treated using H$_2$, O$_2$ and H$_2$/O$_2$ plasma atmospheres.[187] PEEK samples exhibited low contact angles ($\sim$0–3°) after plasma treatment in O$_2$ and H$_2$/O$_2$ atmospheres. Chemical changes on the PEEK surface were characterised by FTIR and XPS:

- In H$_2$ plasma, the oxygen double bond was converted into OH– groups.
- In O$_2$ plasma, –COO– surface bonds have formed.
- In H$_2$/O$_2$ plasma, –COOH surface bonds have formed in addition to the –COO– groups.

It was reported that plasma treatment did not alter the mechanical properties of the treated PEEK surface.[187] Specifically, treatment in O$_2$ plasma reduced the contact angle from 76 to 6°, with FTIR analysis confirming an increase in surface hydroxyl group concentration.[188] Lower contact angles with a hydrophilic threshold of 40° are generally preferred.[189]

Another study demonstrated that the hydrophilic properties of plasma-treated PEEK are reversible, with the contact angle increasing up to 74° after 7 days.[188] The underlying mechanisms of this recovery are complex. One conclusion from the published results is that the –OH groups on the plasma-treated surface become passivated‡‡‡‡‡‡‡‡ during storage. FTIR analysis showed a decrease in the absorption peak intensity corresponding to the –OH groups. The primary explanation for this recovery is the diffusion of hydrophobic oligomers from the PEEK bulk to the surface.[190]

Another innovative solution to maintain the hydrophilic properties of plasma-treated PEEK is surface functionalisation through cross-linking groups or polymers.[188] In one study, a PEG-silane coating was applied to plasma-treated PEEK, with the PEG-silane molecules attached to the –OH groups on the surface. The resulting PEEK–PEG–silane surface exhibited a contact angle of approximately 28°, which changed by less than 20% after 48 days of storage.

Four competing processes were observed in the PEEK–PEG–silane samples:

1. A rapid increase in –OH and –NH$_2$ surface group concentrations after plasma treatment and functionalisation.

2. A rapid decrease in the concentrations of –CH$_2$/–CH$_3$ groups of hydrophobic complexes after plasma treatment and functionalisation.

3. A decrease in –OH and –NH$_2$ surface group concentrations during storage.

4. An increase in –CH$_2$/–CH$_3$ group concentrations during storage.

XPS analysis of both plasma-treated PEEK and PEEK–PEG–silane samples showed a reduction in the C/O ratio. After long-term storage, XPS also revealed decreases in the concentrations of C–O, O–C=O, and C–OH groups. Overall, the use of a silane coupling agent effectively helped preserve the hydrophilic properties of PEEK over time.[188]

A novel approach for PEEK functionalisation by polydopamine§§§§§§§§ (PDA) and chlorhexidine¶¶¶¶¶¶¶¶ (CLX) has also been developed. Initially, the PEEK surface was treated with O$_2$ plasma,[190] and then the samples were immersed in an alkali solution containing a dopamine/chlorhexidine mixture. The resulting PEEK-PDA-CLX surfaces were characterised by

---

‡‡‡‡‡‡‡‡ A process by which reactive surface sites become chemically stabilised, often through the formation of a thin protective layer or by bonding with functional groups, reducing surface reactivity over time.

§§§§§§§§ A bioinspired polymer derived from dopamine, used to functionalise surfaces and enhance biocompatibility.

¶¶¶¶¶¶¶¶ A cationic antimicrobial agent commonly used in medical and dental applications, effective against a broad spectrum of bacteria.

contact angle measurements, FTIR, and XPS. FTIR analysis showed variations in peak intensities; however, it indicated no structural changes in PEEK. XPS analysis revealed the formation of –C=O and –OH groups after plasma treatment, while the N 1s and Cl 2p peaks confirmed the formation of a PDA layer and its crosslinking with CLX. Surface roughness increased progressively after each treatment step, with the PEEK-PDA-CLX surface exhibiting a roughness of 390 nm, approximately double that of untreated PEEK (190 nm). The contact angle decreased to 24°, representing a threefold reduction compared to untreated PEEK, and remained highly stable over time. Furthermore, the controlled release of CLX enhanced the antimicrobial properties of the functionalised PEEK samples.[190]

Based on the advantages and limitations of sulphonation, laser, and plasma treatments for PEEK surface modification, it is clear that each method has specific constraints. Sulphonation and laser treatment primarily modify PEEK surface morphology while causing only minor changes to mechanical properties, surface chemistry, and wettability. In contrast, plasma treatment induces significant changes in surface chemistry but may also risk mechanical weakening of the PEEK surface. The improved wettability achieved through plasma treatment typically requires stabilisation *via* subsequent functionalisation. A combined approach using laser or sulphonation together with plasma treatment, followed by polymerisation/functionalisation, appears to be a promising strategy for producing stable, bioactive PEEK surfaces for biomedical applications. Recent studies support the effectiveness of such combinations.[191,192] Sulphonation created a microporous PEEK surface with a low contact angle due to etching in sulphuric acid.[191] Similarly, combining laser and plasma treatments enhanced both wettability and adhesion properties of PEEK.[192] XPS analysis revealed that samples prepared using these combined methods exhibit the highest concentrations of –OH and –O–C=O groups, indicating improved surface functionalisation.[191,192] It is notable that while plasma treatment has been shown to improve wettability, in the case of Ti–6Al–4V it was found that steam sterilisation performed after plasma treatment led to rapid wettability loss over time without a change in surface roughness.[193]

Beyond these modifications, further surface functionalisation strategies have been developed to introduce specific chemical groups or bioactive layers. Examples include amination (PEEK-NH$_2$) and cyanation (PEEK-NCO) to provide reactive sites for biochemical coupling; fibronectin functionalisation (PEEK-FN) to promote cell adhesion; thin hydroxyapatite coatings (PEEK-HA) for osteoconductivity; titanium or zirconium alkoxide/*tert*-butoxide layers; Ti/TiO$_2$ coatings to enhance osseointegration; and diamond-like carbon coatings to improve wear resistance and reduce bacterial adhesion.[194]

3.7. Antimicrobial functionalisation of implant surfaces

One of the significant drawbacks of PEEK as a cranial implant material is its lack of intrinsic antibacterial properties,

increasing the risk of bacterial infection after implantation.[14,154] Even with substantial material and technological improvements, cranioplasty today remains associated with intra- and postoperative complications, including infection and implant rejection, wound dehiscence and poor soft tissue healing, implant failure due to mechanical stress or bone resorption‖‖‖‖‖‖‖‖, suboptimal osseointegration and bone flap resorption, neurological complications such as seizures and new or worsening deficits, and intracranial complications such as hydrocephalus*********, intracranial haemorrhage, cerebral oedema††††††††, external fluid collections, and subdural hygromas‡‡‡‡‡‡‡‡.[195–197] Most studies report complication rates ranging from 12.1% to 36.6%[5–16] with infection as the leading cause,[17] and a mortality rate ranging from 0.5% to 3.2%.[5,12,13] However, complication rates as high as 50% have been observed for autografts due to bone resorption.[198] While the most common route of antibiotic administration in cranioplasty is intravenous,[199] which is highly effective, and the success rate is independent of the type of antibiotic,[199] long-term use of systemic antibiotics can lead to serious complications, including acute hepatic failure,[200] nephrotoxicity,[201] bacterial resistance,[202] and in severe cases fungal infections like candidiasis,[203] among others. *In situ* sustained-release antibiotic delivery systems can ensure the release of the drug in the desired place of action. Delivery systems can maintain therapeutically effective drug levels at the possible infection site, minimising systemic side effects while effectively localising and decreasing the infection level.[204]

Infection remains a major reason for complications following cranioplasty, particularly when bioinert implants such as PEEK are used. Bioinert materials lack intrinsic antibacterial properties and may promote bacterial adhesion and biofilm formation. To mitigate this risk, diverse antimicrobial strategies have been developed to functionalise the surfaces of bioinert implants. These strategies can be broadly categorised into eight types: drug-loaded surface functionalisation, noble metal-implanted surface functionalisation§§§§§§§§, polymer-functionalised surface modification¶¶¶¶¶¶¶¶, anodised/oxidised/ion-implanted surface functionalisation‖‖‖‖‖‖‖‖, UV-activatable surface functionalisation**********, nanoscale

---

‖‖‖‖‖‖‖‖ Bone resorption is the gradual loss or breakdown of the bone tissue that was implanted, leading to weakening or failure of the graft.

********* A condition characterised by an abnormal accumulation of cerebrospinal fluid within the brain's ventricles.

†††††††† Swelling of brain tissue caused by the accumulation of excess fluid.

‡‡‡‡‡‡‡‡ A fluid-filled cavity, typically resulting from trauma or surgery.

§§§§§§§§ Involves embedding noble metals such as silver into the surface to exert bactericidal effects.

¶¶¶¶¶¶¶¶ Utilises antimicrobial polymer coatings such as chitosan and polyethylene glycol to resist bacterial adhesion.

‖‖‖‖‖‖‖‖ Modified with bioactive ions (*e.g.*, Zn, F, and Cu) *via* anodic oxidation or implantation to enhance antibacterial activity through ion release.

********* Coated with photocatalytic materials (*e.g.*, TiO$_2$) that, upon ultraviolet light exposure, generate reactive oxygen species that kill bacteria.

surface functionalisation†††††††††, nitride surface functionalisation‡‡‡‡‡‡‡‡‡‡, and antimicrobial peptide surface functionalisation§§§§§§§§§§.[205]

The incorporation of drugs into/onto PEEK remains challenging due to its chemical inertness, hydrophobicity, high crystallinity, and non-porous structure. Additionally, the high melting temperature of PEEK ($>220\ °C$) precludes melt-based loading without drug decomposition, consequentially forcing the drug-loading of PEEK to be carried out after 3D printing. To overcome these challenges, the surface of PEEK after 3D printing can be modified by plasma treatment¶¶¶¶¶¶¶¶¶¶, sulphonation, or acid etching‖‖‖‖‖‖‖‖‖‖‖ to increase the surface affinity towards osseointegration, drug molecules and various coatings.[206] Various surface modifications of PEEK have been carried out to create an antibiotic sustained-release system[207–210] and to enhance osseointegration.[153,207,209,210] However, there has been little focus on the potential alteration of the polymer's mechanical properties, which could result from drug–polymer interactions, changes in the amorphous-to-crystalline ratio, the influence of auxiliary materials such as solvents, or variations in coating thickness, *etc.* For instance, it has been demonstrated that the thickness of the cranial implant influences the mechanical performance of the implant-skull system.[54]

As discussed earlier, replacing long-term systemic antibiotic use – associated with complications such as toxicity and resistance – with sustained-release antimicrobial-loaded implants is highly desirable. While drug-loading is one of the most effective strategies, its clinical efficacy is often limited due to the rapid burst release of antibiotics,[211–213] which can evoke bacterial resistance. Furthermore, the onset of post-cranioplasty infection has been reported up to 174 days post-surgery, with a median onset at 24 days,[214] highlighting the need for antimicrobial strategies with long duration of efficacy. This sets an additional limitation to the clinical efficacy of drug-loaded implants due to the rapid decline of antibiotic release (*e.g.*, amikacin, amoxicillin, cefazolin, cephalothin, gentamicin, minocycline, tetracycline, tobramycin, and vancomycin)*********** below the minimal inhibitory concentration†††††††††† within days.[205,211,212,215,216] A possible solution might involve the development of interactive implant surfaces capable of pH-dependent or infection-triggered drug release.

Direct soaking‡‡‡‡‡‡‡‡‡‡‡ of unmodified PEEK in antibiotic solutions typically results in poor drug loading.[217,218] To overcome this, a variety of coating techniques – applied with or without surface modification – have been investigated. These vary in both the choice of antibiotic and the application method.[207–209] For example, a natural antibacterial totarol§§§§§§§§§§§ coating has been successfully applied on an FFF 3D-printed PEEK implant surface.[219] Bioactive composite coatings such as hydroxyapatite-silica¶¶¶¶¶¶¶¶¶¶¶ can be applied *via* spin-spray-coating‖‖‖‖‖‖‖‖‖‖‖‖ to enhance osseointegration.[220] Alternatively, rod-like ZnO nanoarrays can be grown on the PEEK surface (covered with layers of TiO_2) to enable direct absorption of antibiotic agents for antimicrobial functionality.[208]

Sustained-release antibacterial coatings have been demonstrated on PDA-modified PEEK – prepared *via* soaking – by loading them with combinations such as carboxymethyl chitosan–minocycline,[221] chondroitin sulphate–levofloxacin,[222] and osteogenic growth peptide–moxifloxacin hydrochloride in which case the PEEK surface was additionally modified by sulphonation************.[207] Dip coating the PEEK surface was demonstrated with ampicillin and vancomycin, which were previously mixed with a binder (*i.e.* poly lactic-*co*-glycolic acid).[223]

Although drug release profiles and antimicrobial efficacy are frequently reported, the effects of such surface modifications on the mechanical and physical properties of PEEK have been either minimally investigated or remain entirely unexplored. This represents a critical gap in the literature, particularly considering the mechanical demands of cranial implants.

In situ sustained-release antibiotic delivery in cranioplasty can be broadly classified into three categories: release from the bulk material, release from surface coatings, and release from porous surface fillings. Although incorporating drugs directly into the bulk of PEEK is not feasible, drug loading into a post-processed porous surface or into applied surface coatings remains promising. Because of the novelty of *in situ* antibiotic release strategies for PEEK cranial implants and the limited available data, insights can be drawn from established orthopaedic practice. One such example is CERAMENT® BONE VOID FILLER, developed by BoneSupport (Sweden), a biphasic

---

††††††††† Engineered with nanostructures or nanoparticles (*e.g.*, Ag) to enhance antimicrobial activity.

‡‡‡‡‡‡‡‡‡‡ Modified with nitride compounds (*e.g.*, TiN), which may exhibit antibacterial properties by reducing bacterial adhesion through low surface reactivity.

§§§§§§§§§§ Functionalised with covalently bound peptides (*e.g.*, GL13K) that disrupt bacterial membranes, inhibit biofilm formation, and offer broad-spectrum antimicrobial activity.

¶¶¶¶¶¶¶¶¶¶ Plasma treatment is a surface modification technique that uses ionised gas (plasma) to alter the surface properties.

‖‖‖‖‖‖‖‖‖‖‖ Acid etching is a surface treatment method where strong acids are applied to chemically roughen and modify the surface.

*********** Aminoglycosides – amikacin, gentamicin, and tobramycin; β-lactams – amoxicillin (penicillin class), cefazolin (1st gen. cephalosporin), and cephalothin (1st gen. cephalosporin); tetracyclines – minocycline (semisynthetic) and tetracycline (natural); glycopeptide – vancomycin.

†††††††††† The lowest concentration of an antimicrobial agent that prevents visible growth of a microorganism after a specified incubation period.

---

‡‡‡‡‡‡‡‡‡‡‡ A surface modification method where implant materials are immersed in antimicrobial solutions to enable passive drug adsorption onto the surface.

§§§§§§§§§§§ A natural diterpenoid phenol extracted from the heartwood of *Podocarpus totara* and related species, known for its broad-spectrum antibacterial and antioxidant properties.

¶¶¶¶¶¶¶¶¶¶¶ A composite biomaterial combining hydroxyapatite and silica, enhancing bioactivity and mechanical strength in implants.

‖‖‖‖‖‖‖‖‖‖‖‖ A surface modification technique where a liquid coating is sprayed onto a spinning substrate for uniform thin-film deposition.

************ A chemical surface modification technique that introduces sulphonic acid groups onto implant materials, enhancing surface hydrophilicity and chemical reactivity and increasing surface porosity to promote better bone integration.

injectable material composed of 40% HA and 60% calcium sulphate with a liquid component forming a paste. This product has been shown to be a viable alternative to autografts and allografts for the treatment of solid benign tumours and bone cysts in both animals and human patients.[224–226] Two antibiotics have been incorporated into this paste, namely gentamycin (CERAMENT® G) and vancomycin (CERAMENT® V), which were evaluated *via* drug release in patients with hip fracture.[227,228] The drug release was governed by microporosity, diffusion and dissolution, reaching local concentrations 500 times greater than the MIC (2 mg L^{-1} for vancomycin and 4 mg L^{-1} for gentamycin) during the first six hours post-surgery and 200 times greater for at least 60 hours with probable effective levels above the MIC sustained for weeks. Importantly, systemic concentrations remained below toxic thresholds at all times (below the MIC). Furthermore, various ceramic biocomposites as biodegradable antibiotic carriers in the treatment of bone infections were compared, and CERAMENT® G was reported with one of the lowest infection recurrence (4/100) and the lowest wound leak rate (4%).[229] Translating such approaches to cranioplasty, coating PEEK cranial implants with similar biphasic mixtures could provide effective local antimicrobial protection. However, these systems remain relatively uncontrolled, with limited flexibility to adapt antibiotic release kinetics to the variable timelines of cranial bone healing, particularly beyond the initial burst phase. To address this, emerging biomaterials research is exploring more sophisticated strategies for *in situ* antibiotic delivery systems. Stimuli-responsive hydrogel systems have gained traction because of their injectability, conformability, and the possibility to achieve spatiotemporally tunable release profiles.[230,231] Such systems can be engineered to respond to microenvironmental cues such as pH shifts, enzymatic activity, or bacterial metabolites, enabling "on-demand" release of antibiotics when infection risk is highest. For example, these hydrogels could be integrated into sulphonated porous PEEK surfaces or applied as functionalised coatings. While this strategy may reduce unnecessary exposure and preserve antibiotic efficacy, an open question remains regarding the fate of unreleased antibiotics if complete release does not happen. Ideally, hydrogel carriers should be engineered to degrade over time to ensure that any residual antibiotic does not remain trapped within the implant interface.

3.8. Sterilisation

Prior to cranioplasty, cranial implants must undergo sterilisation to prevent postoperative infections. Commonly used methods include chemical sterilisation using ethylene oxide, gamma irradiation, and steam sterilisation *via* autoclaving. Other techniques under investigation include hydrogen peroxide gas plasma, peracetic acid, ozone treatment, and electron beam sterilisation.[232,233] Different materials respond differently to these methods depending on their thermal, chemical, and structural properties, so the selection of the sterilisation technique must be matched to the implant material. For instance, clinically applied 3D-printed PEEK cranial implants have been successfully sterilised using ethylene oxide and steam autoclaving.[51] Due to PEEK's high thermal stability and excellent chemical resistance, it tolerates autoclaving conditions well – typically performed at 121 °C or 134 °C and approximately 2 or 3 bar pressure, respectively[232] – with clinically acceptable accuracy of under 1.00 mm dimensional deformation.[62] Furthermore, PEEK has demonstrated exceptional resistance to radiation, withstanding gamma and electron beam exposure up to 600 kGy,[194,234] making it a viable candidate for these sterilisation methods as well. While the type of sterilisation is important, the number of sterilisation cycles should also be considered. For instance, it has been demonstrated that multiple steam sterilisation of 3D-printed surgical items may lead to the statistical divergence of important mechanical properties such as the hardness and Young's modulus.[235]

Sterilisation is typically the final post-processing step before a cranial implant is surgically implanted. However, the emergence of antimicrobial and antibiotic coatings for PEEK implants introduces a challenge, as many of these coatings are sensitive to heat, radiation, or chemicals used in conventional sterilisation processes. To address this, some studies have applied coatings under aseptic conditions following implant sterilisation,[209] thereby avoiding a second sterilisation step that might degrade the coating. An alternative approach could involve the development of sterilisation-compatible, drug-loaded formulations, in which antibiotics are embedded within heat-stable or radiation-resistant matrices – allowing antimicrobial functionality to be retained following sterilisation. Despite this, many publications do not specify whether, or how, the coated implants were sterilised prior to *in vivo* application, which presents a translational limitation. Ensuring coating efficacy while maintaining sterility remains a critical hurdle in the clinical adoption of antibiotic-coated PEEK cranial implants.

3.9. Outlook and future perspectives

With herein described properties for PEEK cranial implants, being characterised and tested throughout the whole production line as a potential candidate for human use, other new ideas for functionalisation of PEEK keep emerging as we speak. The osteogenic properties of PEEK may, *e.g.*, be enhanced by a substitution reaction with fluorine gas, resulting in a fluorinated PEEK surface, possibly replicating a since long used technique of hydrofluoric acid etching of dental implants.[236,237] Altered properties of the PEEK implant may serve as a ground structure for new tissue engineering initiatives. The combination of materials with PEEK is an exciting and promising way forward to functional materials as shown in a recent paper where the metatarsophalangeal joint of the foot was addressed.[238] Ultrahigh-molecular-weight polyethylene (UHMWPE) was combined with hyaluronic acid into a 3D-printed PEEK scaffold. In this potential small prosthesis, the wear problem was addressed by the constant lubrication of emerging hyaluronic acid within the UHMWPE matrix onto the surface of the prosthesis joint. This example serves as a fine example where additive manufacturing of PEEK implants may become important in the future of reconstructive medicine.

Looking ahead, the development of PEEK-based cranial implants is moving beyond simply replicating the mechanical properties of the skull. The key challenge – and opportunity – lies in designing implants that actively interact with the biological environment, supporting bone regeneration, reducing the risk of infection, and responding to changes in the patient's skull over time. Future implants are expected to integrate multiple surface engineering strategies, such as micro- and nano-scale texturing *via* laser or chemical treatments combined with plasma-induced chemical functionalisation. This approach could make implants to be both mechanically compatible and biologically active, providing surfaces that facilitate cell adhesion, proliferation, and tissue integration.

Antimicrobial strategies will also be an important consideration. Conventional drug-loaded implants often release antibiotics too rapidly, leaving patients at risk of infection once local concentrations decline. Next-generation implants may include responsive coatings that release antibiotics in a controlled manner in response to specific infection-related cues, such as changes in pH or bacterial metabolites. When combined with osteoinductive coatings, like hydroxyapatite or bioactive peptides, these implants could simultaneously promote bone growth and limit infection.

Another promising direction is the use of advanced monitoring and predictive tools. High-resolution imaging, surface chemistry analysis, and computational modelling can guide the design of implants tailored to each patient's specific skull anatomy and mechanical environment. Over time, such strategies may allow implants to better accommodate post-surgical bone remodelling or age-related changes, moving closer to truly personalised cranial reconstruction.

For these innovations to be translated successfully into clinical practice, functionalisation methods must be compatible with sterilisation and long-term storage, and coatings must remain stable over the implant's lifetime. Addressing these challenges could result in cranial implants that are not only mechanically reliable but also biologically active, capable of supporting tissue integration, reducing infection risk, and assisting in the healing process. The convergence of surface engineering, biomaterials science, and responsive drug-delivery systems points to a new generation of cranial implants that go beyond structural restoration, offering active support for patient recovery.

Conclusion

Developing cranial implants that combine favourable antimicrobial release with optimal mechanical performance represents a highly promising avenue for treating cranial bone defects and infections. Although, to date, no clinical cases of cranioplasty using such multifunctional PEEK implants have been reported, current research highlights their strong potential.

This review underscores the crucial importance of matching the mechanical and physical properties of cranial implants to those of cranial bone and the surrounding soft tissues, as mismatches can lead to stress concentrations, implant failure, or impaired healing. A persistent limitation in the field is the frequent comparison of FDM 3D-printed PEEK cranial implant properties with those of femoral cortical bone rather than cranial cortical bone – primarily due to the scarcity of comprehensive cranial bone data. Given that femoral bone differs markedly in structure and loading behaviour, future studies should prioritise region-specific mechanical characterisation of cranial bone.

Even when cranial bone properties are used for comparison, they are typically averaged across the cranial vault or derived from unspecified regions, overlooking significant regional variations in mechanical characteristics.

Furthermore, while extensive research has investigated how FDM printing parameters influence PEEK's mechanical properties, key knowledge gaps remain – particularly across less-studied parameter combinations and printer-specific variations. Similarly, the mechanical implications of surface modification and drug-loading strategies remain insufficiently explored.

Future work should therefore focus on:
- Comprehensive, region-resolved mapping of cranial bone mechanics;
- Systematic evaluation of how FDM parameters affect PEEK's anisotropy and reproducibility;
- Mechanical and physicochemical testing of surface-modified and drug-loaded PEEK implants;
- Integration of adaptive and multifunctional design principles, including smart antimicrobial coatings and osteoinductive surfaces.

Addressing these gaps will advance PEEK-based cranioplasty from structural repair toward bioactive, patient-specific reconstruction – a key step in the evolution of personalised, regenerative cranial implants.

Author contributions

Zoltán Márk Horváth: writing – original draft, writing – review and editing, methodology, visualization, investigation, data curation; Roman Viter: writing – original draft, writing – review and editing; Oskars Radziņš: conceptualization, writing – review and editing; Andreas Thor: writing – review and editing; Tetiana Kolisnyk: conceptualization, methodology, writing – review and editing; Valentyn Mohylyuk: conceptualization, methodology, supervision, writing – review and editing.

Conflicts of interest

No potential competing interest was reported by the authors.

Data availability

Data are available upon request from the authors.

Acknowledgements

References

1 T. Zegers, M. Ter Laak-Poort, D. Koper, B. Lethaus and P. Kessler, The therapeutic effect of patient-specific implants in cranioplasty, *J. Craniomaxillofac. Surg.*, 2017, **45**(1), 82–86, DOI: 10.1016/j.jcms.2016.10.016.

2 L. Di Cosmo, F. Pellicano, J. E. Choueiri, E. Schifino, R. Stefini and D. Cannizzaro, Meta-analyses of the surgical outcomes using personalized 3D-printed titanium and PEEK vs. standard implants in cranial reconstruction in patients undergoing craniectomy, *Neurosurg. Rev.*, 2025, **48**(1), 312, DOI: 10.1007/s10143-025-03470-9.

3 H. Alqurashi, Z. Khurshid, A. U. Y. Syed, S. Rashid Habib, D. Rokaya and M. S. Zafar, Polyetherketoneketone (PEKK): An emerging biomaterial for oral implants and dental prostheses, *J. Adv. Res.*, 2021, **28**, 87–95, DOI: 10.1016/j.jare.2020.09.004.

4 S. Paszkiewicz, P. Lesiak, K. Walkowiak, I. Irska, K. Miadlicki, M. Krolikowski, E. Piesowicz and P. Figiel, The Mechanical, Thermal, and Biological Properties of Materials Intended for Dental Implants: A Comparison of Three Types of Poly(aryl-ether-ketones) (PEEK and PEKK), *Polymers*, 2023, (18), 15, DOI: 10.3390/polym15183706.

5 M. Zanaty, N. Chalouhi, R. M. Starke, S. W. Clark, C. D. Bovenzi, M. Saigh, E. Schwartz, E. S. Kunkel, A. S. Efthimiadis-Budike, P. Jabbour, R. Dalyai, R. H. Rosenwasser and S. I. Tjoumakaris, Complications following cranioplasty: incidence and predictors in 348 cases, *J. Neurosurg.*, 2015, **123**(1), 182–188, DOI: 10.3171/2014.9.jns14405.

6 L. Lee, J. Ker, B. L. Quah, N. Chou, D. Choy and T. T. Yeo, A retrospective analysis and review of an institution's experience with the complications of cranioplasty, *Br. J. Neurosurg.*, 2013, **27**(5), 629–635, DOI: 10.3109/02688697.2013.815313.

7 A. Moreira-Gonzalez, I. T. Jackson, T. Miyawaki, K. Barakat and V. DiNick, Clinical outcome in cranioplasty: critical review in long-term follow-up, *J. Craniofac. Surg.*, 2003, **14**(2), 144–153, DOI: 10.1097/00001665-200303000-00003.

8 M. R. Gooch, G. E. Gin, T. J. Kenning and J. W. German, Complications of cranioplasty following decompressive craniectomy: analysis of 62 cases, *Neurosurg. Focus*, 2009, **26**(6), E9, DOI: 10.3171/2009.3.focus0962.

9 P. De Bonis, P. Frassanito, A. Mangiola, C. G. Nucci, C. Anile and A. Pompucci, Cranial repair: how complicated is filling a "hole"?, *J Neurotrauma*, 2012, **29**(6), 1071–1076, DOI: 10.1089/neu.2011.2116.

10 V. Chang, P. Hartzfeld, M. Langlois, A. Mahmood and D. Seyfried, Outcomes of cranial repair after craniectomy, *J. Neurosurg.*, 2010, **112**(5), 1120–1124, DOI: 10.3171/2009.6.jns09133.

11 N. Acciarri, G. Palandri, A. Cuoci, A. Valluzzi and G. Lanzino, Cranioplasty in neurosurgery: is there a way to reduce complications, *J. Neurosurg. Sci.*, 2020, **64**(1), 1–15, DOI: 10.23736/S0390-5616.16.03843-1.

12 A. Li, T. D. Azad, A. Veeravagu, I. Bhatti, C. Long, J. K. Ratliff and G. Li, Cranioplasty Complications and Costs: A National Population-Level Analysis Using the MarketScan Longitudinal Database, *World Neurosurg.*, 2017, **102**, 209–220, DOI: 10.1016/j.wneu.2017.03.022.

13 R. E. Armstrong and M. F. Ellis, Determinants of 30-day Morbidity in Adult Cranioplasty: An ACS-NSQIP Analysis of 697 Cases, *Plast Reconstr. Surg. Glob. Open*, 2019, **7**(12), e2562, DOI: 10.1097/GOX.0000000000002562.

14 M. Punchak, L. K. Chung, C. Lagman, T. T. Bui, J. Lazareff, K. Rezzadeh, R. Jarrahy and I. Yang, Outcomes following polyetheretherketone (PEEK) cranioplasty: Systematic review and meta-analysis, *J. Clin. Neurosci.*, 2017, **41**, 30–35, DOI: 10.1016/j.jocn.2017.03.028.

15 L. Liu, L. Shou-Tao, L. Ai-Hua, H. Wen-Bo, C. Wen-Rui, Z. Chao, Y. Yu-Xia, Y. Kun-Shan, L. Han-Jie, Z. Ming-Guang and Z. Hai-Jun, Comparison of complications in cranioplasty with various materials: a systematic review and meta-analysis, *Br. J. Neurosurg.*, 2020, **34**(4), 388–396, DOI: 10.1080/02688697.2020.1742291.

16 A. Thien, N. K. King, B. T. Ang, E. Wang and I. Ng, Comparison of polyetheretherketone and titanium cranioplasty after decompressive craniectomy, *World Neurosurg.*, 2015, **83**(2), 176–180, DOI: 10.1016/j.wneu.2014.06.003.

17 A. Pfnür, D. Tosin, M. Petkov, O. Sharon, B. Mayer, C. R. Wirtz, A. Knoll and A. Pala, Exploring complications following cranioplasty after decompressive hemicraniectomy: A retrospective bicenter assessment of autologous, PMMA and CAD implants, *Neurosurg. Rev.*, 2024, **47**(1), 72, DOI: 10.1007/s10143-024-02309-z.

18 J. P. Poppe, M. Spendel, C. J. Griessenauer, A. Gaggl, W. Wurm and S. Enzinger, Point-of-Care 3-Dimensional-Printed Polyetheretherketone Customized Implants for Cranioplastic Surgery of Large Skull Defects, *Oper Neurosurg.*, 2024, **27**(4), 449–454, DOI: 10.1227/ons.0000000000001154.

19 J. A. Motherway, P. Verschueren, G. Van der Perre, J. Vander Sloten and M. D. Gilchrist, The mechanical properties of cranial bone: The effect of loading rate and cranial sampling position, *J. Biomech.*, 2009, **42**(13), 2129–2135, DOI: 10.1016/j.jbiomech.2009.05.030.

20 P. Jill and P. C. Dechow, Material properties of the human cranial vault and zygoma, *Anat. Rec., Part A*, 2003, **274A**(1), 785–797, DOI: 10.1002/ar.a.10096.

21 R. Gauthier, M. Langer, H. Follet, C. Olivier, P. J. Gouttenoire, L. Helfen, F. Rongieras, D. Mitton and F. Peyrin, 3D micro structural analysis of human cortical bone in paired femoral diaphysis, femoral neck and radial diaphysis, *J. Struct. Biol.*, 2018, **204**(2), 182–190, DOI: 10.1016/j.jsb.2018.08.006.

22 T. W. Sadler, *Langman's Medical Embryology*, Lippincott Williams & Wilkins, 2011, p. 12e.

23 X. Zhai, E. A. Nauman, D. Moryl, R. Lycke and W. W. Chen, The effects of loading-direction and strain-rate on the mechanical behaviors of human frontal skull bone, *J. Mech. Behav. Biomed. Mater.*, 2020, **103**, 103597, DOI: 10.1016/j.jmbbm.2019.103597.

24 K. L. Moore, T. V. N. Persaud and M. G. Torchia, *The Developing Human: Clinically Oriented Embryology*, Elsevier, 10 edn, 2015.

25 M. G. Bixel, K. K. Sivaraj, M. Timmen, V. Mohanakrishnan, A. Aravamudhan, S. Adams, B. I. Koh, H. W. Jeong, K. Kruse, R. Stange and R. H. Adams, Angiogenesis is uncoupled from osteogenesis during calvarial bone regeneration, *Nat. Commun.*, 2024, **15**(1), 4575, DOI: 10.1038/s41467-024-48579-5.

26 A. Aciduman and D. Belen, The earliest document regarding the history of cranioplasty from the Ottoman era, *Surg. Neurol.*, 2007, **68**(3), 349–352, DOI: 10.1016/j.surneu.2006.10.073discussion 352–3.

27 J. van Meekeren, *Heel- en Genees- Konstige Aanmerkkingen*, Casparus Commelijn, 1668.

28 A. Martin, *Philipp Franz von Walther's Leben und Wirken*, 1850, Leipzig.

29 A. Alkhaibary, A. Alharbi, N. Alnefaie, A. Oqalaa Almubarak, A. Aloraidi and S. Khairy, Cranioplasty: A Comprehensive Review of the History, Materials, Surgical Aspects, and Complications, *World Neurosurg.*, 2020, **139**, 445–452, DOI: 10.1016/j.wneu.2020.04.211.

30 A. Sanan and S. J. Haines, Repairing holes in the head: A history of cranioplasty, *Neurosurgery*, 1997, **40**(3), 588–603, DOI: 10.1097/00006123-199703000-00033.

31 A. H. Feroze, G. G. Walmsley, O. Choudhri, H. P. Lorenz, G. A. Grant and M. S. Edwards, Evolution of cranioplasty techniques in neurosurgery: historical review, pediatric considerations, and current trends, *J. Neurosurg.*, 2015, **123**(4), 1098–1107, DOI: 10.3171/2014.11.JNS14622.

32 H. B. Gladstone, M. W. McDermott and D. D. Cooke, Implants for cranioplasty, *Otolaryngologic clinics of North America*, 1995, **28**(2), 381–400.

33 B. Zoltán, T. Gábor and H. István, Substitution of skull defects with methyl acrylate, *Magy. Traumatol. Orthop. Helyreallito Seb.*, 1976, **19**(4), 259–268.

34 C. M. Bonfield, A. R. Kumar and P. C. Gerszten, The history of military cranioplasty, *Neurosurg. Focus*, 2014, **36**(4), E18, DOI: 10.3171/2014.1.FOCUS13504.

35 F. L. Stephens, C. M. Mossop, R. S. Bell, T. Tigno, Jr., M. K. Rosner, A. Kumar, L. E. Moores and R. A. Armonda, Cranioplasty complications following wartime decompressive craniectomy, *Neurosurg. Focus*, 2010, **28**(5), E3, DOI: 10.3171/2010.2.FOCUS1026.

36 A. Ebrahimi, N. Nejadsarvari, H. R. Rasouli and A. Ebrahimi, Warfare-related secondary anterior cranioplasty, *Ann. Maxillofac. Surg.*, 2016, **6**(1), 58–62, DOI: 10.4103/2231-0746.186127.

37 P. Flanigan, V. R. Kshettry and E. C. Benzel, World War II, tantalum, and the evolution of modern cranioplasty technique, *Neurosurg. Focus*, 2014, **36**(4), E22, DOI: 10.3171/2014.2.FOCUS13552.

38 L. R. Williams, K. F. Fan and R. P. Bentley, Custom-made titanium cranioplasty: early and late complications of 151 cranioplasties and review of the literature, *Int. J. Oral Maxillofac. Surg.*, 2015, **44**(5), 599–608, DOI: 10.1016/j.ijom.2014.09.006.

39 I. V. Savchenko and S. V. Stankus, Thermal conductivity and thermal diffusivity of tantalum in the temperature range from 293 to 1800 K, *Thermophys. Aeromech.*, 2009, **15**(4), 679–682, DOI: 10.1007/s11510-008-0017-z.

40 D. Simpson, Titanium in Cranioplasty, *J. Neurosurg.*, 1965, **22**, 292–293, DOI: 10.3171/jns.1965.22.3.0292.

41 D. J. Bonda, S. Manjila, W. R. Selman and D. Dean, The Recent Revolution in the Design and Manufacture of Cranial Implants: Modern Advancements and Future Directions, *Neurosurgery*, 2015, **77**(5), 814–824, DOI: 10.1227/NEU.0000000000000899discussion 824.

42 G. Csókay, T. Würsching, S. Szentpéteri, E. L. Nolden, M. Vaszilkó and S. Bogdán, Páciensspecifikus implantátumok használata arckoponya-rekonstrukció során [The use of patient-specific implants in maxillofacial reconstruction], *Orv. Hetil.*, 2024, **165**(40), 1594–1600, DOI: 10.1556/650.2024.33111.

43 G. Welsch, R. Boyer and E. W. Collings, *Materials Properties Handbook: Titanium Alloys*, ASM International, 1993.

44 D. A. Harris, A. J. Fong, E. P. Buchanan, L. Monson, D. Khechoyan and S. Lam, History of synthetic materials in alloplastic cranioplasty, *Neurosurg. Focus*, 2014, **36**(4), E20, DOI: 10.3171/2014.2.FOCUS13560.

45 J. Jaberi, K. Gambrell, P. Tiwana, C. Madden and R. Finn, Long-term clinical outcome analysis of poly-methyl-methacrylate cranioplasty for large skull defects, *J. Oral Maxillofac. Surg.*, 2013, **71**(2), e81–e88, DOI: 10.1016/j.joms.2012.09.023.

46 W. T. Spence, Form-fitting plastic cranioplasty, *J. Neurosurg.*, 1954, **11**(3), 219–225, DOI: 10.3171/jns.1954.11.3.0219.

47 I. Zaed, A. Cardia and R. Stefini, From Reparative Surgery to Regenerative Surgery: State of the Art of Porous Hydroxyapatite in Cranioplasty, *Int. J. Mol. Sci.*, 2022, **23**(10), 5434, DOI: 10.3390/ijms23105434.

48 S. Lewin, L. Kihlstrom Burenstam Linder, U. Birgersson, S. Gallinetti, J. Aberg, H. Engqvist, C. Persson and C. Ohman-Magi, Monetite-based composite cranial implants demonstrate long-term clinical volumetric balance by concomitant bone formation and degradation, *Acta Biomater.*, 2021, **128**, 502–513, DOI: 10.1016/j.actbio.2021.04.015.

49 D. Vitanovics, O. Major, L. Lovas and P. Banczerowski, Személyre szabott koponyacsontpótlások CAD-CAM technológia felhasználásával [Tailored cranioplasty using CAD-CAM technology], *Ideggyogy Sz*, 2014, **67**(11–12), 390–396.

50 P. Scolozzi, A. Martinez and B. Jaques, Complex orbito-fronto-temporal reconstruction using computer-designed PEEK implant, *J. Craniofac. Surg.*, 2007, **18**(1), 224–228, DOI: 10.1097/01.scs.0000249359.56417.7e.

51 J. Zhang, Y. Su, X. Rao, H. Pang, H. Zhu, L. Liu, L. Chen, D. Li, J. He, J. Peng and Y. Jiang, Additively manufactured

polyether ether ketone (PEEK) skull implant as an alternative to titanium mesh in cranioplasty, *Int. J. Bioprint.*, 2023, **9**(1), 634, DOI: 10.18063/ijb.v9i1.634.

52 P. V. Naser, P. Tsitsopoulos, F. Zacharias, A. M. Castano-Leon, A. Buki, B. Depreitere, T. Van Essen, T. K. Korhonen, H. Mee, I. Hossain, J. Posti, L. Lippa, M. C. Papadopoulos, N. Terpolilli, N. Marklund, O. Petr, P. Toth, T. Luoto, S. M. Krieg, A. W. Unterberg, A. Younsi and European Cranioplasty Survey Group, The current state of cranioplasty in Europe - Results from a European cranioplasty survey, *Brain Spine*, 2025, **5**, 104214, DOI: 10.1016/j.bas.2025.104214.

53 G. J. Kwiecien, N. Sinclair, D. M. Coombs, R. S. Djohan, D. Mihal and J. E. Zins, Long-term Effect of Cranioplasty on Overlying Scalp Atrophy, *Plast Reconstr. Surg. Glob. Open*, 2020, **8**(8), e3031, DOI: 10.1097/GOX.0000000000003031.

54 P. Marcian, N. Narra, L. Borak, J. Chamrad and J. Wolff, Biomechanical performance of cranial implants with different thicknesses and material properties: A finite element study, *Comput. Biol. Med.*, 2019, **109**, 43–52, DOI: 10.1016/j.compbiomed.2019.04.016.

55 M. Yang, Z. Wu, H. Yu and J. Cheng, Reconstruction for diverse fronto-orbital defects with computer-assisted designed and computer-assisted manufactured PEEK implants in one-stage operation: Case reports, *Medicine*, 2021, **100**(40), e27452, DOI: 10.1097/MD.0000000000027452.

56 P. O. Santos, G. P. Carmo, R. J. Alves de Sousa, F. A. O. Fernandes and M. Ptak, Mechanical Strength Study of a Cranial Implant Using Computational Tools, *Appl. Sci.*, 2022, **12**(2), 878, DOI: 10.3390/app12020878.

57 M. Niinomi and M. Nakai, Titanium-Based Biomaterials for Preventing Stress Shielding between Implant Devices and Bone, *Int. J. Biomater.*, 2011, **2011**, 836587, DOI: 10.1155/2011/836587.

58 F. Beainy, C. El Amm, Y. Abousleimane, T. Mapstone, O. Beidas and M. Workman, Biomechanical effects of cranioplasty for defects using autogenous calvarial bone, *J. Craniofac. Surg.*, 2012, **23**(2), e152–e155, DOI: 10.1097/SCS.0b013e31824cdc0d.

59 A. Chmielewska and D. Dean, The role of stiffness-matching in avoiding stress shielding-induced bone loss and stress concentration-induced skeletal reconstruction device failure, *Acta Biomater.*, 2024, **173**, 51–65, DOI: 10.1016/j.actbio.2023.11.011.

60 C. Lin-feng, F. Chen, S. Gatea and H. Ou, PEEK based cranial reconstruction using thermal assisted incremental sheet forming, *Proc. Inst. Mech. Eng., Part B*, 2021, **236**(6–7), 997–1004, DOI: 10.1177/09544054211045904.

61 S. Karmani, The thermal properties of bone and the effects of surgical intervention, *Curr. Orthop.*, 2006, **20**(1), 52–58, DOI: 10.1016/j.cuor.2005.09.011.

62 N. Sharma, J. Zubizarreta-Oteiza, C. Tourbier and F. M. Thieringer, Can Steam Sterilization Affect the Accuracy of Point-of-Care 3D Printed Polyetheretherketone (PEEK)

Customized Cranial Implants? An Investigative Analysis, *J. Clin. Med.*, 2023, **12**(7), 2495, DOI: 10.3390/jcm12072495.

63 Administration, U.S. Food and Drug, Use of International Standard ISO 10993-1, ''Biological evaluation of medical devices – Part 1: Evaluation and testing within a risk management process''. 2023, U.S. Food and Drug Administration: Silver Spring, MD.

64 G. Ryan, A. Pandit and D. P. Apatsidis, Fabrication methods of porous metals for use in orthopaedic applications, *Biomaterials*, 2006, **27**(13), 2651–2670, DOI: 10.1016/j.biomaterials.2005.12.002.

65 G. Schmidmaier, M. Lucke, B. Wildemann, N. P. Haas and M. Raschke, Prophylaxis and treatment of implant-related infections by antibiotic-coated implants: a review, *Injury*, 2006, **37**(Suppl 2), S105–S112, DOI: 10.1016/j.injury.2006.04.016.

66 B. Ondrejova, V. Rajtukova, K. Savrtkova, A. Galajdova, J. Zivcak and R. Hudak, Analysis of MRI Artifacts Induced by Cranial Implants in Phantom Models, *Healthcare*, 2025, (7), 13, DOI: 10.3390/healthcare13070803.

67 L. Winter, F. Seifert, L. Zilberti, M. Murbach and B. Ittermann, MRI-Related Heating of Implants and Devices: A Review, *J. Magn. Reson. Imaging*, 2021, **53**(6), 1646–1665, DOI: 10.1002/jmri.27194.

68 A. Valls-Esteve, P. Lustig-Gainza, N. Adell-Gomez, A. Tejo-Otero, M. Engli-Rueda, E. Julian-Alvarez, O. Navarro-Sureda, F. Fenollosa-Artes, J. Rubio-Palau, L. Krauel and J. Munuera, A state-of-the-art guide about the effects of sterilization processes on 3D-printed materials for surgical planning and medical applications: A comparative study, *Int. J. Bioprint.*, 2023, **9**(5), 756, DOI: 10.18063/ijb.756.

69 I. S. Jeon, M. H. Lee, H.-H. Choi, S. Lee, J. W. Chon, D. J. Chung, J. H. Park and J. Y. Jho, Mechanical Properties and Bioactivity of Polyetheretherketone/Hydroxyapatite/Carbon Fiber Composite Prepared by the Mechanofusion Process, *Polymers*, 2021, **13**(12), 1978, DOI: 10.3390/polym13121978.

70 H. Li, J. Yang, F. Tian, X. Li and S. Dong, Study on the Microstructure of Polyether Ether Ketone Films Irradiated with 170 keV Protons by Grazing Incidence Small Angle X-ray Scattering (GISAXS) Technology, *Polymers*, 2020, **12**(11), 2717, DOI: 10.3390/polym12112717.

71 B. Sariyev, A. Abdikadyr, T. Baitikenov, Y. Anuarbekov, B. Golman and C. Spitas, Thermal properties and mechanical behavior of hot pressed PEEK/graphite thin film laminate composites, *Sci. Rep.*, 2023, **13**(1), 12785, DOI: 10.1038/s41598-023-39905-w.

72 J. Zentgraf, F. Nützel, N. Mühlbauer, U. Schultheiss, M. Grad and T. Schratzenstaller, Surface Treatment of Additively Manufactured Polyetheretherketone (PEEK) by Centrifugal Disc Finishing Process: Identification of the Key Parameters, *Polymers*, 2024, **16**(16), 2348, DOI: 10.3390/polym16162348.

73 B. Michel, *Chapter 7 - Plastics Solutions for Practical Problems, in Thermoplastics and Thermoplastic Composites*, 3rd edn, ed M. Biron, William Andrew Publishing, 2018, p. 883–1038, DOI: 10.1016/B978-0-08-102501-7.00007-2.

74 R. Delille, D. Lesueur, P. Potier, P. Drazetic and E. Markiewicz, Experimental study of the bone behaviour of the human skull bone for the development of a physical head model, *Int. J. Crashworthiness*, 2007, **12**(2), 101–108, DOI: 10.1080/13588260701433081.

75 P. Jill and P. C. Dechow, Material properties of the inner and outer cortical tables of the human parietal bone, *Anat. Rec.*, 2002, **268**(1), 7–15, DOI: 10.1002/ar.10131.

76 S.-G. Christina, M. Obert, R. L. Schilling, S. Harth, H. Traupe, E. R. Gizewski and M. A. Verhoff, Age and gender-dependent bone density changes of the human skull disclosed by high-resolution flat-panel computed tomography, *J. Leg. Med.*, 2011, **125**(3), 417–425, DOI: 10.1007/s00414-010-0544-3.

77 A. R. Zanjanijam, I. Major, J. G. Lyons, U. Lafont and D. M. Devine, Fused Filament Fabrication of PEEK: A Review of Process-Structure-Property Relationships, *Polymers*, 2020, (8), 12, DOI: 10.3390/polym12081665.

78 L. Millis Darryl, in Responses of Musculoskeletal Tissues to Disuse and Remobilization, *Canine Rehabilitation and Physical Therapy*, ed D. Millis and D. Levine, W.B. Saunders: St. Louis, 2014, p. 92–153, DOI: 10.1016/b978-1-4377-0309-2.00007-7.

79 S. A. Naghavi, C. Lin, C. Sun, M. Tamaddon, M. Basiouny, P. Garcia-Souto, S. Taylor, J. Hua, D. Li, L. Wang and C. Liu, Stress Shielding and Bone Resorption of Press-Fit Polyether–Ether–Ketone (PEEK) Hip Prosthesis: A Sawbone Model Study, *Polymers*, 2022, **14**(21), 4600, DOI: 10.3390/polym14214600.

80 B. Balani, S. France Chabert, N. Valerie, A. Cantarel and C. Garnier, *Toward improvement of the properties of parts manufactured by FFF (fused filament fabrication) through understanding the influence of temperature and rheological behaviour on the coalescence phenomenon*, 2017, Vol. 1896, p. 040008, DOI: 10.1063/1.5008034.

81 D. J. Blundell and B. N. Osborn, The morphology of poly-(aryl-ether-ether-ketone, *Polymer*, 1983, **24**(8), 953–958, DOI: 10.1016/0032-3861(83)90144-1.

82 K. Abbas, N. Balc, S. Bremen and M. Skupin, Crystallization and Aging Behavior of Polyetheretherketone PEEK within Rapid Tooling and Rubber Molding, *J. Manuf. Mater. Process.*, 2022, **6**(5), 93, DOI: 10.3390/jmmp6050093.

83 M. C. Kuo, C. M. Tsai, J. C. Huang and M. Chen, PEEK composites reinforced by nano-sized SiO2 and Al2O3 particulates, *Mater. Chem. Phys.*, 2005, **90**(1), 185–195, DOI: 10.1016/j.matchemphys.2004.10.009.

84 Z. Huiqing, *Fire -safe polymers and polymer composites*, University of Massachusetts Amherst, United States -- Massachusetts, 2003, p. 289.

85 Y. Kong and J. N. Hay, The measurement of the crystallinity of polymers by DSC, *Polymer*, 2002, **43**(14), 3873–3878, DOI: 10.1016/s0032-3861(02)00235-5.

86 Y. Chuncheng, X. Tian, D. Li, Y. Cao, F. Zhao and C. Shi, Influence of thermal processing conditions in 3D printing on the crystallinity and mechanical properties of PEEK material, *J. Mater. Process. Technol.*, 2017, **248**, 1–7, DOI: 10.1016/j.jmatprotec.2017.04.027.

87 G. J. Farrow, G. H. Wostenholm, M. I. Darby and B. Yates, Thermal expansion of PEEK between 80 and 470K, *J. Mater. Sci. Lett.*, 1990, **9**(6), 743–744, DOI: 10.1007/bf00721820.

88 L. Sharon Xin, P. Cebe and M. Capel, Thermal stability and thermal expansion studies of PEEK and related polyimides, *Polymer*, 1996, **37**(14), 2999–3009, DOI: 10.1016/0032-3861(96)89397-9.

89 H. S. Ranu, The thermal properties of human cortical bone: an in vitro study, *Eng. Med.*, 1987, **16**(3), 175–176, DOI: 10.1243/emed_jour_1987_016_036_02.

90 K. Kashmari, H. Al Mahmud, S. U. Patil, W. A. Pisani, P. Deshpande, M. Maiaru and G. M. Odegard, Multiscale Process Modeling of Semicrystalline PEEK for Tailored Thermomechanical Properties, *ACS Appl. Eng. Mater.*, 2023, **1**(11), 3167–3177, DOI: 10.1021/acsaenm.3c00586.

91 A. Jérémie, L. Rivière, J. Dandurand, A. Lonjon, E. Dantras and C. Lacabanne, Thermal, mechanical and dielectric behaviour of poly(aryl ether ketone) with low melting temperature, *J. Therm. Anal. Calorim.*, 2019, **135**(4), 2147–2157, DOI: 10.1007/s10973-018-7292-x.

92 S. Biyikli, M. F. Modest and R. Tarr, Measurements of thermal properties for human femora, *J. Biomed. Mater. Res.*, 1986, **20**(9), 1335–1345, DOI: 10.1002/jbm.820200908.

93 United States. Federal Aviation, Administration, Laboratories Battelle Memorial Institute. Columbus, J. Hughes Technical Center William, Defense United States. Department of, Aeronautics United States. National, and Administration Space, Metallic materials properties development and standardization (MMPDS): MMPDS-07, April 2012. MMPDS-07, April 2012. 2012, Federal Aviation Administration, Washington, D.C.

94 K. Chen, W. Liang, Q. Zhu, H. Shen, Y. Yang, Y. Li, H. Li, Y. Wang and R. Qian, Clinical Outcomes After Cranioplasty With Titanium Mesh, Polyetheretherketone, or Composite Bone Cement: A Retrospective Study, *J. Craniofac. Surg.*, 2023, **34**(8), 2246–2251, DOI: 10.1097/SCS.0000000000009542.

95 S. Jan, P. Werner, M. S. P. Shaffer, V. Demchuk, V. Altstädt and A. H. Windle, Carbon-nanofibre-reinforced poly(ether ether ketone) composites, *Composites, Part A*, 2002, **33**(8), 1033–1039, DOI: 10.1016/s1359-835x(02)00084-2.

96 M. N. Uddin, P. S. Dhanasekaran and R. Asmatulu, Mechanical properties of highly porous PEEK bionanocomposites incorporated with carbon and hydroxyapatite nanoparticles for scaffold applications, *Prog Biomater*, 2019, **8**(3), 211–221, DOI: 10.1007/s40204-019-00123-1.

97 Z. Yachen, K. Zhao, Y. Li and F. Chen, Mechanical characterization of biocompatible PEEK by FDM, *J. Manuf. Process.*, 2020, **56**, 28–42, DOI: 10.1016/j.jmapro.2020.04.063.

98 I. Vindokurov, Y. Pirogova, M. Tashkinov and V. V. Silberschmidt, Effect of Heat Treatment on Elastic Properties and Fracture Toughness of Fused Filament Fabricated PEEK for Biomedical Applications, *Polymers*, 2022, **14**(24), 5521, DOI: 10.3390/polym14245521.

99 B. V. Phanindra, Y. Kumar and A. Khanra, Modelling and structural analysis of skull/cranial implant: beyond mid-

line deformities, *Acta Bioeng. Biomech.*, 2017, 19, DOI: 10.5277/ABB-00547-2016-04.

100 S. Prabaha, B. Tej Challa and S. Kumar Gummadi, A comprehensive analysis on the processing-structure-property relationships of FDM-based 3-D printed poly-etheretherketone (PEEK) structures, *Materialia*, 2022, 22, DOI: 10.1016/j.mtla.2022.101427.

101 B. Sourabh, D. L. Subit, G. R. Paskoff, B. S. Shender, J. R. Crandall and R. S. Salzar, Influence of bone micro-structure on the mechanical properties of skull cortical bone – A combined experimental and computational approach, *J. Mech. Behav. Biomed. Mater.*, 2017, **65**, 688–704, DOI: 10.1016/j.jmbbm.2016.09.041.

102 A. Audrey, R. Delille, D. Lesueur, K. Bruyère, C. Masson and P. Drazétic, Geometrical and material parameters to assess the macroscopic mechanical behaviour of fresh cranial bone samples, *J. Biomech.*, 2014, **47**(5), 1180–1185, DOI: 10.1016/j.jbiomech.2013.10.060.

103 Z. He, H. He, J. Lou, Y. Li, D. Li, Y. Chen and S. Liu, Fabrication, Structure and Mechanical and Ultrasonic Properties of Medical Ti6Al4V Alloys Part I: Microstructure and Mechanical Properties of Ti6Al4V Alloys Suitable for Ultrasonic Scalpel, *Materials*, 2020, (2), 13, DOI: 10.3390/ma13020478.

104 T. Devrim, M. Güngörürler, H. Havıtçıoğlu and Y. Arman, Investigation of effective coating of the Ti–6Al–4V alloy and 316L stainless steel with graphene or carbon nanotubes with finite element methods, *J. Mater. Res. Technol.*, 2020, **9**(6), 15880–15893, DOI: 10.1016/j.jmrt.2020.11.052.

105 A. Fitch David, B. K. Hoffmeister and J. de Ana, Ultrasonic evaluation of polyether ether ketone and carbon fiber-reinforced PEEK, *J. Mater. Sci.*, 2010, **45**(14), 3768–3777, DOI: 10.1007/s10853-010-4428-1.

106 D. Garcia-Gonzalez, M. Rodriguez-Millan, A. Rusinek and A. Arias, Low temperature effect on impact energy absorption capability of PEEK composites, *Compos. Struct.*, 2015, **134**, 440–449, DOI: 10.1016/j.compstruct.2015.08.090.

107 P. J. Rae, E. N. Brown and E. B. Orler, The mechanical properties of poly(ether-ether-ketone) (PEEK) with emphasis on the large compressive strain response, *Polymer*, 2007, **48**(2), 598–615, DOI: 10.1016/j.polymer.2006.11.032.

108 A. Alvaredo-Atienza, J. P. Fernandez-Blazquez, P. Castell and R. Guzman de Villoria, Production of graphene nanoplate/polyetheretherketone composites by semi-industrial melt-compounding, *Heliyon*, 2020, **6**(4), e03740, DOI: 10.1016/j.heliyon.2020.e03740.

109 J. H. McElhaney, J. L. Fogle, J. W. Melvin, R. R. Haynes, V. L. Roberts and N. M. Alem, Mechanical properties on cranial bone, *J. Biomech.*, 1970, **3**(5), 495–511, DOI: 10.1016/0021-9290(70)90059-x.

110 M. Freedman, M. Ring and L. F. Stassen, Effect of alveolar bone support on zygomatic implants in an extra-sinus position–a finite element analysis study, *Int. J. Oral Maxillofac. Surg.*, 2015, **44**(6), 785–790, DOI: 10.1016/j.ijom.2015.01.009.

111 G. Liu, N. Hu, J. Huang, Q. Tu and F. Xu, Experimental Investigation on the Mechanical and Dynamic Thermomechanical Properties of Polyether Ether Ketone Based on Fused Deposition Modeling, *Polymers*, 2024, (21), 16, DOI: 10.3390/polym16213007.

112 A. D. Brown, K. A. Rafaels and T. Weerasooriya, Shear behavior of human skull bones, *J. Mech. Behav. Biomed. Mater.*, 2021, **116**, 104343, DOI: 10.1016/j.jmbbm.2021.104343.

113 J. Prashant, S. Shiva Sai Bharadwaja, S. Rattra, C. Vipin Gupta, P. Breedon, Y. Reinwald and M. Juneja, Designing cranial fixture shapes and topologies for optimizing PEEK implant thickness in cranioplasty, *Proc. Inst. Mech. Eng., Part L*, 2023, **237**(8), 1752–1770, DOI: 10.1177/14644207231155761.

114 S. H. Mian, K. Moiduddin, S. M. Elseufy and H. Alkhalefah, Adaptive Mechanism for Designing a Personalized Cranial Implant and Its 3D Printing Using PEEK, *Polymers*, 2022, (6), 14, DOI: 10.3390/polym14061266.

115 K. Moiduddin, S. H. Mian, S. M. Elseufy, H. Alkhalefah, S. Ramalingam and A. Sayeed, Polyether-Ether-Ketone (PEEK) and Its 3D-Printed Quantitate Assessment in Cranial Reconstruction, *J. Funct. Biomater.*, 2023, **14**(8), 429, DOI: 10.3390/jfb14080429.

116 R. K. Nalla, J. H. Kinney and R. O. Ritchie, Mechanistic fracture criteria for the failure of human cortical bone, *Nat. Mater.*, 2003, **2**(3), 164–168, DOI: 10.1038/nmat832.

117 E. Launey Maximilien, M. J. Buehler and R. O. Ritchie, On the Mechanistic Origins of Toughness in Bone, *Annu. Rev. Mater. Res.*, 2010, **40**(1), 25–53, DOI: 10.1146/annurev-matsci-070909-104427.

118 Z. Zhong Pu, Z. Peng Liao, N. Yoda, W. Li, K. Sasaki, G. Hong, M. V. Swain and Q. Li, XFEM Fracture Modelling for Implant-Supported Fixed Partial Dentures, *Appl. Mech. Mater.*, 2016, **846**, 488–493, DOI: 10.4028/www.scientific.net/AMM.846.488.

119 F. P. Moncayo-Matute, E. Vazquez-Silva, P. G. Pena-Tapia, P. B. Torres-Jara, D. P. Moya-Loaiza and T. J. Viloria-Avila, Finite Element Analysis of Patient-Specific 3D-Printed Cranial Implant Manufactured with PMMA and PEEK: A Mechanical Comparative Study, *Polymers*, 2023, (17), 15, DOI: 10.3390/polym15173620.

120 A. Al-Ahmari, E. A. Nasr, K. Moiduddin, S. Anwar, M. A. Kindi and A. Kamrani, A comparative study on the customized design of mandibular reconstruction plates using finite element method, *Adv. Mech. Eng.*, 2015, 7(7), DOI: 10.1177/1687814015593890.

121 J. C. Wall, S. K. Chatterji and J. W. Jeffery, Age-related changes in the density and tensile strength of human femoral cortical bone, *Calcif. Tissue Int.*, 1979, **27**(2), 105–108, DOI: 10.1007/BF02441170.

122 L. F. Lozano, M. A. Peña-Rico, A. Heredia, J. Ocotlán-Flores, A. Gómez-Cortés, R. Velázquez, I. A. Belío and L. Bucio, Thermal analysis study of human bone, *J. Mater. Sci.*, 2003, **38**(23), 4777–4782, DOI: 10.1023/a:1027483220584.

123 G. B. Reinish and A. S. Nowick, Effect of Moisture on the Electrical Properties of Bone, *J. Electrochem. Soc.*, 2019, **123**(10), 1451–1455, DOI: 10.1149/1.2132617.

124 S. Singh and S. Saha, Electrical Properties of Bone: A Review, *Clin. Orthop. Relat. Res.*, 1984, 186.

125 X. N. Dong and X. E. Guo, The dependence of transversely isotropic elasticity of human femoral cortical bone on porosity, *J. Biomech.*, 2004, **37**(8), 1281–1287, DOI: 10.1016/j.jbiomech.2003.12.011.

126 H. H. Bayraktar, E. F. Morgan, G. L. Niebur, G. E. Morris, E. K. Wong and T. M. Keaveny, Comparison of the elastic and yield properties of human femoral trabecular and cortical bone tissue, *J. Biomech.*, 2004, **37**(1), 27–35, DOI: 10.1016/s0021-9290(03)00257-4.

127 M. Bittner-Frank, A. G. Reisinger, O. G. Andriotis, D. H. Pahr and P. J. Thurner, Cortical and trabecular mechanical properties in the femoral neck vary differently with changes in bone mineral density, *JBMR Plus*, 2024, **8**(6), ziae049, DOI: 10.1093/jbmrpl/ziae049.

128 S. Vijayavenkataraman, W. C. Yan, W. F. Lu, C. H. Wang and J. Y. H. Fuh, 3D bioprinting of tissues and organs for regenerative medicine, *Adv. Drug Delivery Rev.*, 2018, **132**, 296–332, DOI: 10.1016/j.addr.2018.07.004.

129 S. S. Crump, *Apparatus and method for creating three-dimensional objects*. 1992, Google Patents.

130 A. MohanaSundaram, Y. Kamalakannan, V. Raja, M. Mofatteh and M. A. Haque, The World's first 3D-printed PEEK cranial implant: a new horizon in precision and personalized neurosurgery, *Neurosurg. Rev.*, 2024, **47**(1), 616, DOI: 10.1007/s10143-024-02867-2.

131 N. Alasseri and A. Alasraj, Patient-specific implants for maxillofacial defects: challenges and solutions, *Maxillofac. Plast Reconstr. Surg.*, 2020, **42**(1), 15, DOI: 10.1186/s40902-020-00262-7.

132 C. N. T. Kim, X. B. Cao, T. D. Vu and V. T. Thang, Design and mechanical evaluation of a large cranial implant and fixation parts, *Interdiscip. Neurosurg.*, 2023, 31, DOI: 10.1016/j.inat.2022.101676.

133 S. C. Chang, G. Tobias, A. K. Roy, C. A. Vacanti and L. J. Bonassar, Tissue engineering of autologous cartilage for craniofacial reconstruction by injection molding, *Plast Reconstr. Surg.*, 2003, **112**(3), 793–799, DOI: 10.1097/01.PRS.0000069711.31021.94discussion 800–1.

134 C. Ian, D. Bourell and I. Gibson, Additive manufacturing: rapid prototyping comes of age, *Rapid Prototyping J.*, 2012, **18**(4), 255–258, DOI: 10.1108/13552541211231563.

135 P. Honigmann, N. Sharma, B. Okolo, U. Popp, B. Msallem and F. M. Thieringer, Patient-Specific Surgical Implants Made of 3D Printed PEEK: Material, Technology, and Scope of Surgical Application, *BioMed Res. Int.*, 2018, **2018**, 4520636, DOI: 10.1155/2018/4520636.

136 N. Sharma, S. Aghlmandi, F. Dalcanale, D. Seiler, H. F. Zeilhofer, P. Honigmann and F. M. Thieringer, Quantitative Assessment of Point-of-Care 3D-Printed Patient-Specific Polyetheretherketone (PEEK) Cranial Implants, *Int. J. Mol. Sci.*, 2021, **22**(16), 8521, DOI: 10.3390/ijms22168521.

137 G. Peng, J. Zhao, W. Wu, W. Ye, Y. Wang, S. Wang and S. Zhang, Effects of extrusion speed and printing speed on the 3D printing stability of extruded PEEK filament, *J. Manuf. Process.*, 2019, **37**, 266–273, DOI: 10.1016/j.jmapro.2018.11.023.

138 C. Cleiton André, R. Davies, H. van der Pol and O. Ghita, PEEK filament characteristics before and after extrusion within fused filament fabrication process, *J. Mater. Sci.*, 2022, **57**(1), 766–788, DOI: 10.1007/s10853-021-06652-0.

139 E. B. Hughes, J. Alfarone, E. S. Chernov, N. A. Debick, M. Jalal, Y. Kim, A. Suryadevara and S. Krishnamurthy, Polyetheretherketone (PEEK) Into the Future: Lowering Infection Rates in Cranioplasty, *Cureus*, 2024, **16**(10), e72060, DOI: 10.7759/cureus.72060.

140 P. Wang, Z. Bin, X. Hongchuan, D. Shouling and H. Chuanzhen, Effects of printing parameters of fused deposition modeling on mechanical properties, surface quality, and microstructure of PEEK, *J. Mater. Process. Technol.*, 2019, **271**, 62–74, DOI: 10.1016/j.jmatprotec.2019.03.016.

141 D. J. Jaekel, D. W. MacDonald and S. M. Kurtz, Characterization of PEEK biomaterials using the small punch test, *J. Mech. Behav. Biomed. Mater.*, 2011, **4**(7), 1275–1282, DOI: 10.1016/j.jmbbm.2011.04.014.

142 Y. Sonaye Surendrasingh, P. M. Jason, T. Kwek-Tze, J. S. Owusu-Danquah and P. Sikder, A comprehensive analysis of high-temperature material extrusion 3D printing parameters on fracture patterns and strength of polyetheretherketone cranial implants, *Prog. Addit. Manuf.*, 2024, **10**(1), 927–942, DOI: 10.1007/s40964-024-00688-9.

143 W. Peng, B. Zou and S. Ding, Modeling of surface roughness based on heat transfer considering diffusion among deposition filaments for FDM 3D printing heat-resistant resin, *Appl. Therm. Eng.*, 2019, 161, DOI: 10.1016/j.applthermaleng.2019.114064.

144 M. F. Arif, S. Kumar, K. M. Varadarajan and W. J. Cantwell, Performance of biocompatible PEEK processed by fused deposition additive manufacturing, *Mater. Des.*, 2018, **146**, 249–259, DOI: 10.1016/j.matdes.2018.03.015.

145 D. Shouling, B. Zou, P. Wang and H. Ding, Effects of nozzle temperature and building orientation on mechanical properties and microstructure of PEEK and PEI printed by 3D-FDM, *Polym. Test.*, 2019, 78, DOI: 10.1016/j.polymertesting.2019.105948.

146 R. Marianna, T. Ghidini, F. Cecchini, A. Brandao and F. Nanni, Additive layer manufacturing of poly (ether ether ketone) via FDM, *Composites, Part B*, 2018, **145**, 162–172, DOI: 10.1016/j.compositesb.2018.03.029.

147 P. G. Alves, L. Guilherme Abreu de Paula, J. Jonathan Rubio Arias, E. Gervasoni Chaves and M. de Fátima Vieira Marques, Comparative analysis of poly(ether-ether-ketone) properties aged in different conditions for application in pipelines, *J. Therm. Anal. Calorim.*, 2022, **148**(1), 79–95, DOI: 10.1007/s10973-022-11582-3.

148 B. Pidhatika, V. T. Widyaya, P. C. Nalam, Y. A. Swasono and R. Ardhani, Surface Modifications of High-Performance Polymer Polyetheretherketone (PEEK) to Improve Its Biological Performance in Dentistry, *Polymers*, 2022, (24), 14, DOI: 10.3390/polym14245526.

149 S. Thulung, K. Ranabhat, S. Bishokarma and D. N. Gongal, Morphometric Measurement of Cranial Vault Thickness: A Tertiary Hospital Based Study, *J. Nepal Med. Assoc.*, 2019, **57**(215), 29–32, DOI: 10.31729/jnma.3949.

150 J. Persson, B. Helgason, H. Engvist, S. J. Ferguson and C. Persson, Stiffness and strength of cranioplastic implant systems in comparison to cranial bone, *J. Craniomaxillofac. Surg.*, 2018, **46**(3), 418–423, DOI: 10.1016/j.jcms.2017.11.025.

151 J. Zwirner, S. Safavi, M. Scholze, K. C. Li, J. N. Waddell, B. Busse, B. Ondruschka and N. Hammer, Topographical mapping of the mechanical characteristics of the human neurocranium considering the role of individual layers, *Sci. Rep.*, 2021, **11**(1), 3721, DOI: 10.1038/s41598-020-80548-y.

152 X. Han, N. Sharma, Z. Xu, L. Scheideler, J. Geis-Gerstorfer, F. Rupp, F. M. Thieringer and S. Spintzyk, An In Vitro Study of Osteoblast Response on Fused-Filament Fabrication 3D Printed PEEK for Dental and Cranio-Maxillofacial Implants, *J. Clin. Med.*, 2019, **8**(6), 771, DOI: 10.3390/jcm8060771.

153 Y. Zhao, H. M. Wong, W. Wang, P. Li, Z. Xu, E. Y. Chong, C. H. Yan, K. W. Yeung and P. K. Chu, Cytocompatibility, osseointegration, and bioactivity of three-dimensional porous and nanostructured network on polyetheretherketone, *Biomaterials*, 2013, **34**(37), 9264–9277, DOI: 10.1016/j.biomaterials.2013.08.071.

154 Y. Chen, L. Zhang, T. Qin, Z. Wang, Y. Li and B. Gu, Evaluation of neurosurgical implant infection rates and associated pathogens: evidence from 1118 postoperative infections, *Neurosurg. Focus*, 2019, **47**(2), E6, DOI: 10.3171/2019.5.FOCUS18582.

155 J. Zhang, W. Tian, J. Chen, J. Yu, J. Zhang and J. Chen, The application of polyetheretherketone (PEEK) implants in cranioplasty, *Brain Res. Bull.*, 2019, **153**, 143–149, DOI: 10.1016/j.brainresbull.2019.08.010.

156 P. R. Schmidlin, B. Stawarczyk, M. Wieland, T. Attin, C. H. Hammerle and J. Fischer, Effect of different surface pre-treatments and luting materials on shear bond strength to PEEK, *Dent. Mater.*, 2010, **26**(6), 553–559, DOI: 10.1016/j.dental.2010.02.003.

157 Y. Chen, W. Liu, Z. Wu, S. Wang, Y. Li, B. Su and S. Li, Advantages and feasibility of prefabricated PEEK crowns for aesthetic restoration in primary teeth, *Sci. Rep.*, 2024, **14**(1), 28398, DOI: 10.1038/s41598-024-79306-1.

158 I. Caglar, S. M. Ates and Z. Yesil Duymus, An In Vitro Evaluation of the Effect of Various Adhesives and Surface Treatments on Bond Strength of Resin Cement to Polyetheretherketone, *J Prosthodont*, 2019, **28**(1), e342–e349, DOI: 10.1111/jopr.12791.

159 S. Sunpreet, C. Prakash, H. Wang, X.-F. Yu and S. Ramakrishna, Plasma treatment of polyether-ether-ketone: A means of obtaining desirable biomedical characteristics, *Eur. Polym. J.*, 2019, **118**, 561–577, DOI: 10.1016/j.eurpolymj.2019.06.030.

160 T. Konrad, A. Ewa Wiącek and M. Jurak, Influence of nitrogen plasma treatment on the wettability of polyetheretherketone and deposited chitosan layers, *Adv. Polym. Technol.*, 2017, **37**(6), 1557–1569, DOI: 10.1002/adv.21813.

161 X. Han, N. Sharma, S. Spintzyk, Y. Zhou, Z. Xu, F. M. Thieringer and F. Rupp, Tailoring the biologic responses of 3D printed PEEK medical implants by plasma functionalization, *Dent. Mater.*, 2022, **38**(7), 1083–1098, DOI: 10.1016/j.dental.2022.04.026.

162 G. Qiuying, S. Zhang, Z. Hu, L. Gao, H. Li, J. Yang and L. Zhu, Surface modification of PEEK fabric via UV irradiation, air plasma, and oxygen plasma: Effects on adhesion to epoxy resin, *Surf. Interfaces*, 2025, **67**, DOI: 10.1016/j.surfin.2025.106644.

163 G. Primc, Strategies for Improved Wettability of Polyetheretherketone (PEEK) Polymers by Non-Equilibrium Plasma Treatment, *Polymers*, 2022, **14**(23), 5319, DOI: 10.3390/polym14235319.

164 A. Elisa, J. Holtmannspötter, T. Hofmann and H.-J. Gudladt, Vacuum-UV of polyetheretherketone (PEEK) as a surface pre-treatment for structural adhesive bonding, *J. Adhesion*, 2018, **96**(10), 917–944, DOI: 10.1080/00218464.2018.1545646.

165 Z. Yanyan, L. Liu, Y. Ma, L. Xiao and Y. Liu, Enhanced Osteoblasts Responses to Surface-Sulfonated Polyetheretherketone via a Single-Step Ultraviolet-Initiated Graft Polymerization, *Ind. Eng. Chem. Res.*, 2018, **57**(31), 10403–10410, DOI: 10.1021/acs.iecr.8b02158.

166 J. Khoury, I. Selezneva, S. Pestov, V. Tarassov, A. Ermakov, A. Mikheev, M. Lazov, S. R. Kirkpatrick, D. Shashkov and A. Smolkov, Surface bioactivation of PEEK by neutral atom beam technology, *Bioact. Mater.*, 2019, **4**, 132–141, DOI: 10.1016/j.bioactmat.2019.02.001.

167 A. Kirkpatrick, S. Kirkpatrick, M. Walsh, S. Chau, M. Mack, S. Harrison, R. Svrluga and J. Khoury, Investigation of accelerated neutral atom beams created from gas cluster ion beams, *Nucl. Instrum. Methods Phys. Res., Sect. B*, 2013, **307**, 281–289, DOI: 10.1016/j.nimb.2012.11.084.

168 Z. Huan, V. K. Goel and S. B. Bhaduri, A fast route to modify biopolymer surface: A study on polyetheretherketone (PEEK), *Mater. Lett.*, 2014, **125**, 96–98, DOI: 10.1016/j.matlet.2014.03.130.

169 P. Sikder, C. R. Grice, B. Lin, V. K. Goel and S. B. Bhaduri, Single-Phase, Antibacterial Trimagnesium Phosphate Hydrate Coatings on Polyetheretherketone (PEEK) Implants by Rapid Microwave Irradiation Technique, *ACS Biomater. Sci. Eng.*, 2018, **4**(8), 2767–2783, DOI: 10.1021/acsbiomaterials.8b00594.

170 M. Chen, L. Ouyang, T. Lu, H. Wang, F. Meng, Y. Yang, C. Ning, J. Ma and X. Liu, Enhanced Bioactivity and Bacteriostasis of Surface Fluorinated Polyetheretherketone, *ACS Appl. Mater. Interfaces*, 2017, **9**(20), 16824–16833, DOI: 10.1021/acsami.7b02521.

171 S. Chayanun, T. Chanamuangkon, B. Boonsuth, A. R. Boccaccini and B. Lohwongwatana, Enhancing PEEK surface bioactivity: Investigating the effects of combining sulfonation with sub-millimeter laser machining, *Mater. Today Bio*, 2023, **22**, 100754, DOI: 10.1016/j.mtbio.2023.100754.

172 Y. Shi, T. Deng, Y. Peng, Z. Qin, M. Ramalingam, Y. Pan, C. Chen, F. Zhao, L. Cheng and J. Liu, Effect of Surface Modification of PEEK Artificial Phalanx by 3D Printing on its Biological Activity, *Coatings*, 2023, **13**(2), 400, DOI: 10.3390/coatings13020400.

173 M. Xie, G. Y. Xiao, Z. G. Song and Y. P. Lu, The Formation Process and Mechanism of the 3D Porous Network on the Sulfonated PEEK Surface, *ACS Appl. Mater. Interfaces*, 2024, **16**(11), 13585–13596, DOI: 10.1021/acsami.4c00055.

174 B. Asik and O. Y. Ozyilmaz, Effects of various laser applications on surface roughness and bond strength to veneering composites of polyether ether ketone (PEEK) and polyether ketone ketone (PEKK) materials, *Lasers Med. Sci.*, 2024, **39**(1), 269, DOI: 10.1007/s10103-024-04213-w.

175 F. Turkkal, A. K. Culhaoglu and V. Sahin, Composite-veneering of polyether-ether-ketone (PEEK): evaluating the effects of different surface modification methods on surface roughness, wettability, and bond strength, *Lasers Med. Sci.*, 2023, **38**(1), 95, DOI: 10.1007/s10103-023-03749-7.

176 H. Tsuka, K. Morita, K. Kato, H. Kimura, H. Abekura, I. Hirata, K. Kato and K. Tsuga, Effect of laser groove treatment on shear bond strength of resin-based luting agent to polyetheretherketone (PEEK), *J. Prosthodont. Res.*, 2019, **63**(1), 52–57, DOI: 10.1016/j.jpor.2018.08.001.

177 F. Luo, R. Mao, Y. Huang, L. Wang, Y. Lai, X. Zhu, Y. Fan, K. Wang and X. Zhang, Femtosecond laser optimization of PEEK: efficient bioactivity achieved by synergistic surface chemistry and structures, *J. Mater. Chem. B.*, 2022, **10**(36), 7014–7029, DOI: 10.1039/d2tb01142e.

178 L. Wei, T. Wanless, S. H. Foulger, I. Gnilitskyi and I. Luzinov, Modulation of Polyether Ether Ketone (PEEK) Surfaces via High-Speed Femtosecond Laser Treatment and Perfluoropolyether-Based Polyurethane Coating, *ACS Appl. Mater. Interfaces*, 2025, **17**(32), 46353–46362, DOI: 10.1021/acsami.5c09732.

179 Z. Junliang, C. Li, X. Xue, Y. Yan and X. Sedao, Experiment and simulation of femtosecond laser processing of peek materials: One-step laser optimization of friction performance and wettability, *Opt. Laser Technol.*, 2025, **183**, DOI: 10.1016/j.optlastec.2024.112320.

180 S. H. Um, J. Lee, M. Chae, C. Paternoster, F. Copes, P. Chevallier, D. H. Lee, S. W. Hwang, Y. C. Kim, H. S. Han, K. S. Lee, D. Mantovani and H. Jeon, Biomedical Device Surface Treatment by Laser-Driven Hydroxyapatite Penetration-Synthesis Technique for Gapless PEEK-to-Bone Integration, *Adv. Healthcare Mater.*, 2024, **13**(26), e2401260, DOI: 10.1002/adhm.202401260.

181 A. Riveiro, R. Soto, R. Comesaña, M. Boutinguiza, J. del Val, F. Quintero, F. Lusquiños and J. Pou, Laser surface modification of PEEK, *Appl. Surf. Sci.*, 2012, **258**(23), 9437–9442, DOI: 10.1016/j.apsusc.2012.01.154.

182 W. Xue, P. Zou, Z. Yang, J. Xu and H. Miao, Surface damage and modification analysis of CF/PEEK under laser irradiation based on experiments and molecular dynamics, *Polym. Compos.*, 2025, **46**(14), 12875–12891, DOI: 10.1002/pc.29904.

183 Z. Weixuan, K. Gao, X. Li, J. Liao and G. Li, Dual surface modification of medical-grade PEEK: Nanosecond laser pre-treatment and hydrothermal hydroxyapatite coating, *Opt. Laser Technol.*, 2025, **191**, DOI: 10.1016/j.optlastec.2025.113307.

184 L. Qingtao, D. Wei, J. Lv, Z. Wang, Z. Xu, P. Yang, Y. Zhang and C. Li, Enhancing interfacial bond strength between PEEK and inkjet-printed silver film through laser surface modification for additive manufacturing of electronics, *J. Mater. Res. Technol.*, 2024, **30**, 6724–6736, DOI: 10.1016/j.jmrt.2024.05.007.

185 G. Primc and M. Mozetic, Surface Modification of Polymers by Plasma Treatment for Appropriate Adhesion of Coatings, *Materials*, 2024, (7), 17, DOI: 10.3390/ma17071494.

186 A. K. Ahmad, R. Le-Franc, J.-P. Guin and J.-F. Coulon, Investigating the thermal effects of plasma surface treatment on crystallinity and mechanical behavior of PEEK, *Polym. Degrad. Stab.*, 2023, **216**, DOI: 10.1016/j.polymdegradstab.2023.110500.

187 Q. Fu, M. Gabriel, F. Schmidt, W. D. Muller and A. D. Schwitalla, The impact of different low-pressure plasma types on the physical, chemical and biological surface properties of PEEK, *Dent. Mater.*, 2021, **37**(1), e15–e22, DOI: 10.1016/j.dental.2020.09.020.

188 S. Poonam, M. Sahu, O. Prakash and S. Bhattacharya, Long-term surface modification of PEEK polymer using plasma and PEG silane treatment, *Surf. Interfaces*, 2021, **25**, DOI: 10.1016/j.surfin.2021.101253.

189 V. Rutkunas, R. Borusevicius, E. Balciunas, U. Jasinskyte, M. Alksne, E. Simoliunas, S. Zlatev, V. Ivanova, V. Bukelskiene and E. Mijiritsky, The Effect of UV Treatment on Surface Contact Angle, Fibroblast Cytotoxicity, and Proliferation with Two Types of Zirconia-Based Ceramics, *Int. J. Environ. Res. Public Health*, 2022, **19**(17), 11113, DOI: 10.3390/ijerph191711113.

190 T. Yang, Y. Zhang, Z. Gao and B. Li, Triple-modified PEEK surface via plasma treatment, polydopamine coating and chlorhexidine: Assessment of biocompatibility and antibacterial properties, *Dent. Mater.*, 2025, **41**(6), 730–744, DOI: 10.1016/j.dental.2025.04.004.

191 T. Ma, J. Zhang, X. Liu, S. Sun and J. Wu, Effects of combined modification of sulfonation, oxygen plasma and silane on the bond strength of PEEK to resin, *Dent. Mater.*, 2024, **40**(4), e1–e11, DOI: 10.1016/j.dental.2024.02.001.

192 T. Chen, S. Xu, X. Chen, D. Wang, C. Liu and H. Liu, Effects of Nd: YAG LASER irradiation and O(2) plasma on the adhesive performance of poly-ether-ether-ketone (PEEK), *J. Mech. Behav. Biomed. Mater.*, 2024, **152**, 106461, DOI: 10.1016/j.jmbbm.2024.106461.

193 P. Trebacz, M. Pawlik, A. Kurkowska, K. Wilk, A. Piatek and M. Czopowicz, Low-Temperature Plasma Activation of Biomaterials and Its Stability over Time and Post-Sterilisation Effects, *Materials*, 2026, (3), 19, DOI: 10.3390/ma19030643.

194 I. V. Panayotov, V. Orti, F. Cuisinier and J. Yachouh, Polyetheretherketone (PEEK) for medical applications,

J. Mater. Sci. Mater. Med., 2016, **27**(7), 118, DOI: 10.1007/s10856-016-5731-4.

195 S. I. Khalid, K. B. Thomson, S. Maasarani, A. L. Wiegmann, J. Smith, O. Adogwa, A. I. Mehta and A. H. Dorafshar, Materials Used in Cranial Reconstruction: A Systematic Review and Meta-Analysis, *World Neurosurg.*, 2022, **164**, e945–e963, DOI: 10.1016/j.wneu.2022.05.073.

196 D. Shepetovsky, G. Mezzini and L. Magrassi, Complications of cranioplasty in relationship to traumatic brain injury: a systematic review and meta-analysis, *Neurosurg. Rev.*, 2021, **44**(6), 3125–3142, DOI: 10.1007/s10143-021-01511-7.

197 N. K. Sahoo, K. Tomar, A. Thakral and N. M. Rangan, Complications of Cranioplasty, *J. Craniofac. Surg.*, 2018, **29**(5), 1344–1348, DOI: 10.1097/SCS.0000000000004478.

198 G. A. Grant, M. Jolley, R. G. Ellenbogen, T. S. Roberts, J. R. Gruss and J. D. Loeser, Failure of autologous bone-assisted cranioplasty following decompressive craniectomy in children and adolescents, *J. Neurosurg.*, 2004, **100**(2 Suppl Pediatrics), 163–168, DOI: 10.3171/ped.2004.100.2.0163.

199 Y. Cao, B. Wang, J. Shan, Z. Gong, J. Kuang and Y. Gao, Indirect comparison of efficacy between different antibiotic prophylaxis against the intracranial infection after craniotomy, *Antimicrob. Resist. Infect. Control*, 2020, **9**(1), 122, DOI: 10.1186/s13756-020-00784-9.

200 M. K. Taher, A. Alami, C. A. Gravel, D. Tsui, L. M. Bjerre, F. Momoli, D. R. Mattison and D. Krewski, Systemic quinolones and risk of acute liver failure I: Analysis of data from the US FDA adverse event reporting system, *JGH Open*, 2021, **5**(7), 778–784, DOI: 10.1002/jgh3.12585.

201 M. C. Morales-Alvarez, Nephrotoxicity of Antimicrobials and Antibiotics, *Adv. Chronic Kidney Dis.*, 2020, **27**(1), 31–37, DOI: 10.1053/j.ackd.2019.08.001.

202 N. A. R. Gow, C. Johnson, J. Berman, A. T. Coste, C. A. Cuomo, D. S. Perlin, T. Bicanic, T. S. Harrison, N. Wiederhold, M. Bromley, T. Chiller and K. Edgar, The importance of antimicrobial resistance in medical mycology, *Nat. Commun.*, 2022, **13**(1), 5352, DOI: 10.1038/s41467-022-32249-5.

203 R. A. Drummond, J. V. Desai, E. E. Ricotta, M. Swamydas, C. Deming, S. Conlan, M. Quinones, V. Matei-Rascu, L. Sherif, D. Lecky, C. R. Lee, N. M. Green, N. Collins, A. M. Zelazny, D. R. Prevots, D. Bending, D. Withers, Y. Belkaid, J. A. Segre and M. S. Lionakis, Long-term antibiotic exposure promotes mortality after systemic fungal infection by driving lymphocyte dysfunction and systemic escape of commensal bacteria, *Cell Host Microbe*, 2022, **30**(7), 1020–1033.e6, DOI: 10.1016/j.chom.2022.04.013.

204 G. M. Jantzen and J. R. Robinson, *Sustained-and Controlled-Release Drug-Delivery Systems*, 2002, pp. 747–789, DOI: 10.1201/9780824744694.ch15.

205 J. Grischke, J. Eberhard and M. Stiesch, Antimicrobial dental implant functionalization strategies -A systematic review, *Dent. Mater. J.*, 2016, **35**(4), 545–558, DOI: 10.4012/dmj.2015-314.

206 Z. Zheng, P. Liu, X. Zhang, X. Jingguo, W. Yongjie, X. Zou, X. Mei, S. Zhang and S. Zhang, Strategies to improve bioactive and antibacterial properties of polyetheretherketone (PEEK) for use as orthopedic implants, *Mater. Today Bio*, 2022, **16**, 100402, DOI: 10.1016/j.mtbio.2022.100402.

207 G. Chengzhe, Z. Wang, Z. Jiao, Z. Wu, M. Guo, Y. Wang, J. Liu and P. Zhang, Enhancing antibacterial capability and osseointegration of polyetheretherketone (PEEK) implants by dual-functional surface modification, *Mater. Des.*, 2021, **205**, DOI: 10.1016/j.matdes.2021.109733.

208 N. C. Lau, Y. C. Lai, D. W. Chen and K. W. Cheng, Antibacterial Activity Studies of 3D-Printing Polyetheretherketone Substrates with Surface Growth of 2D TiO(2)/ZnO Rodlike Arrays, *ACS Omega*, 2022, **7**(11), 9559–9572, DOI: 10.1021/acsomega.1c06931.

209 Z. Xue, Z. Wang, A. Sun, J. Huang, W. Wu, M. Chen, X. Hao, Z. Huang, X. Lin and S. Weng, Rapid construction of polyetheretherketone (PEEK) biological implants incorporated with brushite (CaHPO(4).2H(2)O) and antibiotics for anti-infection and enhanced osseointegration, *Mater. Sci. Eng. C*, 2020, **111**, 110782, DOI: 10.1016/j.msec.2020.110782.

210 X. Xiaojie, J. Zuo, H. Zeng, Y. Zhao and Z. Fan, Improving Osseointegration Potential of 3D Printed PEEK Implants with Biomimetic Periodontal Ligament Fiber Hydrogel Surface Modifications, *Adv. Funct. Mater.*, 2023, **34**(14), 2308811, DOI: 10.1002/adfm.202308811.

211 J. A. Jennings, D. P. Carpenter, K. S. Troxel, K. E. Beenken, M. S. Smeltzer, H. S. Courtney and W. O. Haggard, Novel Antibiotic-loaded Point-of-care Implant Coating Inhibits Biofilm, *Clin. Orthop. Relat. Res.*, 2015, **473**(7), 2270–2282, DOI: 10.1007/s11999-014-4130-8.

212 N. J. Hickok, I. M. Shapiro and A. F. Chen, The Impact of Incorporating Antimicrobials into Implant Surfaces, *J. Dent. Res.*, 2018, **97**(1), 14–22, DOI: 10.1177/0022034517731768.

213 J. S. Price, A. F. Tencer, D. M. Arm and G. A. Bohach, Controlled release of antibiotics from coated orthopedic implants, *J. Biomed. Mater. Res.*, 1996, **30**(3), 281–286, DOI: 10.1002/(sici)1097-4636(199603)30:3 < 281::Aid-jbm2 > 3.0.Co;2-m.

214 M. Ha, J. H. Lee, H. J. Choi, B. C. Kim and S. Yu, Postoperative infection after cranioplasty in traumatic brain injury: a single center experience, *J. Trauma Inj.*, 2022, **35**(4), 255–260, DOI: 10.20408/jti.2022.0043.

215 C. Shyi-Tien, H.-W. Chien, C.-Y. Cheng, H.-M. Huang, T.-Y. Song, Y.-C. Chen, C.-H. Wu, Y.-H. Hsueh, Y.-H. Wang and S.-F. Ou, Drug-release dynamics and antibacterial activities of chitosan/cefazolin coatings on Ti implants, *Prog. Org. Coat.*, 2021, **159**, DOI: 10.1016/j.porgcoat.2021.106385.

216 U. Brohede, J. Forsgren, S. Roos, A. Mihranyan, H. Engqvist and M. Stromme, Multifunctional implant coatings providing possibilities for fast antibiotics loading with subsequent slow release, *J. Mater. Sci. Mater. Med.*, 2009, **20**(9), 1859–1867, DOI: 10.1007/s10856-009-3749-6.

217 J. Sundblom, S. Gallinetti, U. Birgersson, H. Engqvist and L. Kihlstrom, Gentamicin loading of calcium phosphate implants: implications for cranioplasty, *Acta Neurochir.*, 2019, **161**(6), 1255–1259, DOI: 10.1007/s00701-019-03895-4.

218 D. W. Chen, K. Y. Lee, M. H. Tsai, T. Y. Lin, C. H. Chen and K. W. Cheng, Antibacterial Application on Staphylococcus aureus Using Antibiotic Agent/Zinc Oxide Nanorod Arrays/Polyethylethylketone Composite Samples, *Nanomaterials*, 2019, **9**(5), 713, DOI: 10.3390/nano9050713.

219 X. Han, N. Sharma, Z. Xu, S. Krajewski, P. Li, S. Spintzyk, L. Lv, Y. Zhou, F. M. Thieringer and F. Rupp, A balance of biocompatibility and antibacterial capability of 3D printed PEEK implants with natural totarol coating, *Dent. Mater.*, 2024, **40**(4), 674–688, DOI: 10.1016/j.dental.2024.02.011.

220 T. Frankenberger, C. L. Graw, N. Engel, T. Gerber, B. Frerich and M. Dau, Sustainable Surface Modification of Polyetheretherketone (PEEK) Implants by Hydroxyapatite/Silica Coating-An In Vivo Animal Study, *Materials*, 2021, **14**(16), 4589, DOI: 10.3390/ma14164589.

221 Y. Zhang, L. Zhang, Y. Zhang, P. Yu, Q. Hu, Y. Liu and Y. Zheng, Concentration-Optimized Minocycline-Modified Antimicrobial Coatings on Polyetheretherketone for the Prevention of Implant-Associated Infections, *Coatings*, 2025, **15**(6), 622, DOI: 10.3390/coatings15060622.

222 M. Li, J. Liu, Y. Li, W. Chen, Z. Yang, Y. Zou, Y. Liu, Y. Lu and J. Cao, Enhanced osteogenesis and antibacterial activity of dual-functional PEEK implants via biomimetic polydopamine modification with chondroitin sulfate and levofloxacin, *J. Biomater. Sci. Polym. Ed.*, 2024, **35**(18), 2790–2806, DOI: 10.1080/09205063.2024.2390745.

223 N.-C. Lau, M.-H. Tsai, D. W. Chen, C.-H. Chen and K.-W. Cheng, Preparation and Characterization for Antibacterial Activities of 3D Printing Polyetheretherketone Disks Coated with Various Ratios of Ampicillin and Vancomycin Salts, *Appl. Sci.*, 2020, **10**(1), 97, DOI: 10.3390/app10010097.

224 J. Kaczmarczyk, P. Sowinski, M. Goch and K. Katulska, Complete twelve month bone remodeling with a bi-phasic injectable bone substitute in benign bone tumors: a prospective pilot study, *BMC Musculoskeletal Disord.*, 2015, **16**, 369, DOI: 10.1186/s12891-015-0828-3.

225 A. Hofmann, S. Gorbulev, T. Guehring, A. P. Schulz, R. Schupfner, M. Raschke, S. Huber-Wagner, P. M. Rommens and C. ERTiFy Study Group, Autologous Iliac Bone Graft Compared with Biphasic Hydroxyapatite and Calcium Sulfate Cement for the Treatment of Bone Defects in Tibial Plateau Fractures: A Prospective, Randomized, Open-Label, Multicenter Study, *J. Bone Jt. Surg., Am. Vol.*, 2020, **102**(3), 179–193, DOI: 10.2106/JBJS.19.00680.

226 W. Hettwer, P. F. Horstmann, S. Bischoff, D. Gullmar, J. R. Reichenbach, P. S. P. Poh, M. van Griensven, F. Gras and M. Diefenbeck, Establishment and effects of allograft and synthetic bone graft substitute treatment of a critical size metaphyseal bone defect model in the sheep femur, *APMIS*, 2019, **127**(2), 53–63, DOI: 10.1111/apm.12918.

227 M. Stravinskas, M. Nilsson, A. Vitkauskiene, S. Tarasevicius and L. Lidgren, Vancomycin elution from a biphasic ceramic bone substitute, *Bone Joint Res.*, 2019, **8**(2), 49–54, DOI: 10.1302/2046-3758.82.BJR-2018-0174.R2.

228 M. Stravinskas, P. Horstmann, J. Ferguson, W. Hettwer, M. Nilsson, S. Tarasevicius, M. M. Petersen, M. A. McNally and L. Lidgren, Pharmacokinetics of gentamicin eluted from a regenerating bone graft substitute: In vitro and clinical release studies, *Bone Joint Res.*, 2016, **5**(9), 427–435, DOI: 10.1302/2046-3758.59.BJR-2016-0108.R1.

229 J. Ferguson, M. Diefenbeck and M. McNally, Ceramic Biocomposites as Biodegradable Antibiotic Carriers in the Treatment of Bone Infections, *J. Bone Jt. Infect.*, 2017, **2**(1), 38–51, DOI: 10.7150/jbji.17234.

230 S. Akay and A. Yaghmur, Recent Advances in Antibacterial Coatings to Combat Orthopedic Implant-Associated Infections, *Molecules*, 2024, **29**(5), 1172, DOI: 10.3390/molecules29051172.

231 S. Wu, T. Gai, J. Chen, X. Chen and W. Chen, Smart responsive in situ hydrogel systems applied in bone tissue engineering, *Front. Bioeng. Biotechnol.*, 2024, **12**, 1389733, DOI: 10.3389/fbioe.2024.1389733.

232 M. Zaborniak, J. Kluczyński, J. Stańko and T. Ślęzak, The Influence of the Steam Sterilization Process on Selected Properties of Polymer Samples Produced in MEX and JMT Processes, *Materials*, 2024, **17**(23), 5763, DOI: 10.3390/ma17235763.

233 C. Ferreira, D. Sterling, M. Reynolds, K. Dusenbery, C. Chen and P. Alaei, First clinical implementation of GammaTile permanent brain implants after FDA clearance, *Brachytherapy*, 2021, **20**(3), 673–685, DOI: 10.1016/j.brachy.2020.12.005.

234 M. Kurtz Steven, Chapter 6 - Chemical and Radiation Stability of PEEK, in *PEEK Biomaterials Handbook*, ed. S. M. Kurtz, 2012, William Andrew Publishing, Oxford. pp. 75–79, DOI: 10.1016/B978-1-4377-4463-7.10006-5.

235 M. Antonowicz-Hupsch, P. Trebacz, L. A. Piras, A. Piatek, A. Auguscik, K. Cholewa, W. Groelich, M. Pawlik, L. Manassero, A. Kurkowska, A. Barteczko, D. Mancusi and M. Czopowicz, Impact of multiple steam sterilizations on the mechanical properties of 3D-printed surgical items, *Sci. Rep.*, 2025, **15**(1), 41688, DOI: 10.1038/s41598-025-25561-9.

236 J. Lyu, X. Dai, Z. Li, D. Zhang, S. Chen, Y. Liu, L. Yu, P. Liu and X. Liu, Unexpected hydrophilicity and bio-selectivity of fluorinated PEEK: enhancing bone regeneration through macrophage and BMSC cooperation, *Mater. Horiz.*, 2025, **12**, 10194–10207, DOI: 10.1039/d5mh00773a.

237 S. F. Lamolle, M. Monjo, M. Rubert, H. J. Haugen, S. P. Lyngstadaas and J. E. Ellingsen, The effect of hydrofluoric acid treatment of titanium surface on nanostructural and chemical changes and the growth of MC3T3-E1 cells, *Biomaterials*, 2009, **30**(5), 736–742, DOI: 10.1016/j.biomaterials.2008.10.052.

238 S. Li, L. Tang, J. Pu, J. Wang, C. Fan, Z. Li and J. Song, Continuous Hyaluronic Acid Supply by a UHMWPE/PEEK Interlocking Scaffold for Metatarsophalangeal Joint Prosthesis Lubricating Applications, *ACS Appl. Mater. Interfaces*, 2025, **17**(8), 11704–11717, DOI: 10.1021/acsami.4c19390.